REPORT DOCUMENTATION PAGE

Form Approved
OMB No. 0704-0188

1. REPORT DATE *(DD-MM-YYYY)*	2. REPORT TYPE	3. DATES COVERED *(From - To)*
19-10-2011	Conference Paper	

4. TITLE AND SUBTITLE

Accuracy and Best Practices for Small-Scale Rocket Engine Testing

5a. CONTRACT NUMBER

5b. GRANT NUMBER

5c. PROGRAM ELEMENT NUMBER

6. AUTHOR(S)
M.D.A. Lightfoot, S.A. Danczyk (AFRL/RZSA),, J.M. Watts (Orbital Sciences), and S.A. Schumaker (AFRL/RZSA)

5d. PROJECT NUMBER

5f. WORK UNIT NUMBER
50260538

7. PERFORMING ORGANIZATION NAME(S) AND ADDRESS(ES)

Air Force Research Laboratory (AFMC)
AFRL/RZSA
10 E. Saturn Blvd.
Edwards AFB CA 93524-7680

8. PERFORMING ORGANIZATION REPORT NUMBER

AFRL-RZ-ED-TP-2011-420

9. SPONSORING / MONITORING AGENCY NAME(S) AND ADDRESS(ES)

Air Force Research Laboratory (AFMC)
AFRL/RZS
5 Pollux Drive
Edwards AFB CA 93524-7048

10. SPONSOR/MONITOR'S ACRONYM(S)

11. SPONSOR/MONITOR'S NUMBER(S)
AFRL-RZ-ED-TP-2011-420

12. DISTRIBUTION / AVAILABILITY STATEMENT

Approved for public release; distribution unlimited (PA #11884).

13. SUPPLEMENTARY NOTES
For presentation at the JANNAF 2011 Joint Subcommittee Meeting, Huntsville, AL, 5-9 Dec 2011.

14. ABSTRACT

An in-depth analysis of the uncertainties associated with small-scale rocket engine testing has been conducted. The analysis uses terminology and approaches detailed in the ISO *'Guide to the Expression of Uncertainty in Measurement'* (GUM) and a recent NASA handbook on the subject (NASA HBK-8739.19-3). Along with this analysis, best practices for minimizing uncertainties are provided. AFRL's Experimental Cell-1 facility is used as the example engine, and the data values provided come from this system. The facility is sized to test a single, full-scale element or an array of scaled-down elements producing thrust in the range of 100-500 pounds. The facility has recently completed an overhaul to increase the number of data channels available and to improve accuracy. The measurand being specifically evaluated is c*-efficiency (η_{c^*}). However, details are given on all of the parameters which contribute to the measurement and calculation of this value. This analysis should aid in the design, upgrade, operation and data assessment of EC-1 and other small-scale facilities.

15. SUBJECT TERMS

16. SECURITY CLASSIFICATION OF:			17. LIMITATION OF ABSTRACT	18. NUMBER OF PAGES	19a. NAME OF RESPONSIBLE PERSON
					Dr. M.D.A. Lightfoot
a. REPORT	b. ABSTRACT	c. THIS PAGE	SAR	48	19b. TELEPHONE NUMBER *(include area code)*
Unclassified	**Unclassified**	**Unclassified**			N/A

ACCURACY AND BEST PRACTICES FOR SMALL-SCALE ROCKET ENGINE TESTING

Lightfoot, M.D.A.[1], Danczyk, S.A.[1], Watts, J.M.[2], Schumaker, S.A.[1]

[1]Aerophysics Branch, Propulsion Directorate
Air Force Research Laboratory

[2] Orbital Sciences
Taurus II

ABSTRACT

An in-depth analysis of the uncertainties associated with small-scale rocket engine testing has been conducted. The analysis uses terminology and approaches detailed in the ISO *'Guide to the Expression of Uncertainty in Measurement'* (GUM) and a recent NASA handbook on the subject (NASA HBK-8739.19-3). Along with this analysis, best practices for minimizing uncertainties are provided. AFRL's Experimental Cell-1 facility is used as the example engine, and the data values provided come from this system. The facility is sized to test a single, full-scale element or an array of scaled-down elements producing thrust in the range of 100-500 pounds. The facility has recently completed an overhaul to increase the number of data channels available and to improve accuracy. The measurand being specifically evaluated is c*-efficiency (η_{c^*}). However, details are given on all of the parameters which contribute to the measurement and calculation of this value. This analysis should aid in the design, upgrade, operation and data assessment of EC-1 and other small-scale facilities.

INTRODUCTION

Small-scale engine tests are used for a variety of rocket-engine development programs and tasks. These small-scale tests are more cost-effective than large-scale testing and can be completed in a shorter time frame. Experiments are often used to investigate the effects of new or novel components (or fuels), especially to compare them to the prior state-of-the art. At the end of the experimental series, a judgment is made based on these comparisons; of particular interest is any increase in performance provided by the new component. Good comparisons require reliable data and knowledge of the uncertainties associated with them. This work investigates the uncertainties associated with a small-scale test facility and recommends best practices. The small-scale facility under assessment in this work is the Experimental Cell-1 (EC-1) facility at Edwards AFB [1].

The EC-1 facility has recently undergone a major upgrade in measurement ability and uncertainty reduction. An uncertainty analysis was used to highlight specific areas for improvement. Also, previous experience and the results from the analysis were used to develop some best practice recommendations. Because these recommendations are often based on direct experience, comparisons between prior and current practices will be given when available. While many brand names and models are given throughout this work, their listing does not constitute their endorsement or recommendation. Specifics are provided to give as complete an understanding as possible of EC-1's engine and its associated measurement uncertainty.

There has been an ever-increasing emphasis on uncertainty analysis in recent years throughout many different industries and countries [2-6]. Most publications, such as AIAA, require uncertainty estimation to be included in journal articles. Standards organizations, such as NIST and ISO, have published and updated their recommendations on this topic in recent years [3, 4]. Often, however, journal articles do not follow these recommendations. One reason for this shortcoming is the extreme complexity involved in a thorough uncertainty analysis. Another reason may be that the standard organizations' publications give only a general approach to uncertainty analysis, an approach which is independent of application. This generality allows the main publication (by the ISO), *'Guide to the Expression of*

Uncertainty in Measurement' (GUM), to be widely employed throughout a diversity of industries, but it complicates application to a specific industry and impacts consistent usage in the aerospace industry. NASA has recently published a more targeted handbook on the subject [2] which gives guidance and examples more specifically tailored to aerospace applications. A previous JANNAF publication addressed analysis of test data, but is generally directed to larger test facilities and is currently rather dated [7]; for example, it predates the availability of the CEA code, now in general use for calculating theoretical performance. The intent of this current work is to follow the GUM as much as feasible, which will generally be in line with NIST and NASA recommendations. Many of the specific approaches described in the NASA handbook will be adopted. An attempt is made to be as rigorous as possible in the thorough application of the guidelines, and assumptions and their impacts as well as departures from rigorous approaches are specifically noted. Given the depth of these manuals and complex nature of uncertainty analysis, they will not be summarized here. Familiarity with the subject is assumed in this text, and the reader is referred to the GUM [3] and NASA handbook [2] for additional background.

Many different parameters could be considered when assessing rocket engines and engine components, and small-scale facilities with different focuses have used different parameters [1, 8-11]. Herein emphasis will be placed on c*-efficiency, η_{c^*}, because of its previous usage in EC-1 and common usage in the literature as a performance parameter. c*-efficiency is the ratio of measured characteristic exhaust velocity, c^*, to a theoretical maximum; it is a measure of how effectively the chemical energy of the fuel and oxidizer are converted to useful energy. This efficiency, and c^* itself, cannot be measured directly, so an uncertainty analysis of the various measurements involved in its calculation will be undertaken. Throughout the uncertainty analysis best practices will be identified and areas which could be targeted to further reduce uncertainty will be identified.

Each of the measurements needed to calculate c*-efficiency is given its own section below. These sections are all laid out in a similar fashion, in a manner that follows GUM and NASA recommendations. First, the basic way in which measurements and calibrations are conducted is given. Information on traceability to NIST or ASTM standards, as applicable, is given here. Then, the mathematical formulation for the measurand is given. This equation is often derived from the way calibrations are performed. From the formulation of the measurand, an equation for the combined uncertainty is presented. Each of the singular uncertainty components is discussed in the section following the mathematical formulation. Often these components are, themselves, a combination of many uncertainties. For example, the pressure uncertainty contains the uncertainty in voltage; this voltage uncertainty, in turn, contains uncertainties related to resolution, repeatability and other factors. Throughout these sections, uncertainties are given from an instrument standpoint. The uncertainties in measuring the specific value of interest are not included. So, the uncertainty in the thermocouple itself would be considered but the difference between the average gas temperature and the temperature being measured is not included. These latter differences are discussed briefly in the final subsection where a summary of best practices for lowering uncertainty is provided. Prior to that section, however, values for specific and combined uncertainties are given in tabular form and as a pie chart breaking down the contribution of each subcomponent is shown. In some cases a discussion of lowering the largest remaining contributor to the uncertainty is given. his analysis is still a work in progress. As such, the analysis of degrees of freedom is not fully developed. Where it is obvious, the distribution of the uncertainty and degrees of freedom are listed in the tables. Blank entries have yet to be rigorously considered. Because the distribution and degrees of freedom remain to be assessed, confidence intervals cannot be given. Intervals at 95% will be computed and presented in the future.

The units used throughout this text are a mixture of English and SI standards, particularly temperatures which are given in a mixture of °C and °F. A choice to not convert units was made to reflect how the values are actually reported by the manufacturer and made and recorded during testing. Attention and care should be used when referring to values to ensure they are in the expected units.

NOMENCLATURE

A	Area
AR	Area ratio (chamber to throat)
C	Curve fit parameter
*c**	Characteristic exhaust velocity
C_D	Discharge Coefficient
C_{FF}	Critical flow factor
C%	Carbon percentage
cov	Covariance
D	Diameter
H%	Hydrogen percentage
j	Mass of contaminant in the sample
m	*M*ass
$\dot{m}$.	Mass flow rate
MR	*M*ixture ratio
MW	Molecular weight (of Hydrogen or Carbon)
P	Pressure
R	Gas constant
r	Radius
s	Correction to C_FF due to velocity
S	Sensitivity coefficients
T	Temperature
t	Time
u	Uncertainty
V	Voltage
W	Width
x	Stoichiometric parameter for carbon
y	Stoichiometric parameter for hydrogen
η_{c^*}	Efficiency (characteristic exhaust velocity)
ΔH	Enthalpy (heat)
ρ	Density

Subscripts

atm	Atmospheric
c	Chamber
C	Carbon
CO2	Carbon dioxide
comb	Combustion
cw	From catch-and-weigh
f	Formation
fuel	Fuel (or liquid)
H	Hydrogen
H2O	Water
jun	Junction box
meas	Measured
ox	Oxidizer (or gas)
p	Pipe
R	Reactants
record	Recorded by DAQ system
sn	Sonic nozzle throat
supply	Set/supplied by calibration source
t	Throat
tc	Thermocouple
theo	Theoretical (calculated via CEA)
total	Total
ven	Venturi
v	Vapor

UNCERTAINTY ANALYSIS

C*-EFFICIENCY

BASIC PROCEDURE

Because η_{c^*} is the end result of engine testing, this section gives basic details of the EC-1 facility in which testing is performed. This engine test facility typically operates with heat-sink hardware composed of several engine sections. Each section has a square inner cross-section and either a round or square outer cross-section and is either 1 or 2 inches in length. The inner cross-section is either 1 inch per side with a negligible rounding at the corners (0.01 inch or less) or 2 inches per side with 0.25 inch radii at the corners; the outer diameter is 4.5 inches or it is 4.5 inches on a side if square. The material is oxygen-free copper. The nozzle is water-cooled and also constructed of oxygen-free copper. Figure 1 shows a photograph of the engine. General ranges and typical operating conditions are given in Table 1. Specific details of facility operation are given throughout the text below when important or illustrative.

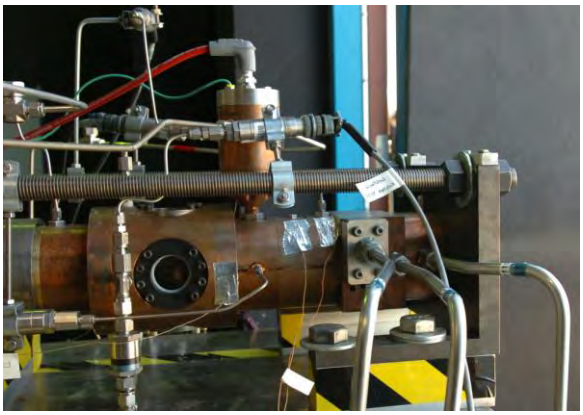

Figure 1. Picture of the EC-1 facility engine.

Parameter	Typical Values
Fuel	RP-2
Chamber Pressure	100-800 psi
Reactant Temperature	40-100° F
Atmospheric Pressure	13.2-13.6 psi
Thrust	100-500 lb
Nozzle Throat Diameter	0.45-0.65 inch
Area Ratio (A_c/A_t)	3-25
Sonic Nozzle Diameter	0.07-0.20 inch
Cavitating Venturi Throat	0.031-0.050 inch

Table 1. The typical operating conditions in the EC-1 facility motor. This is the range of conditions considered in the analysis.

MATHEMATICAL FORMULATION

The parameter of interest, the overall measurand, is c*-efficiency, η_{c*}. The equation for η_{c*} is

$$\eta_{c*} = c^*_{meas}/c^*_{theo} \tag{1}$$

where

$$c^*_{actual} = \frac{P_c A_t}{\dot{m}_{total}} \tag{2}$$

c^*_{theo} is calculated using the CEA code [12]. Neither the measured nor theoretical c^* is available directly.

Initially, it appears that c^*_{meas} depends only on measurements of the chamber pressure, throat area and total mass flow rate. However, as explained below, these measurements can be affected by other measured parameters, such as temperature. Uncertainties in the measurement of each contributing parameter will be considered in separate subsections.

Temperature is also an important measurand because the heat loss of the engine is not directly measured because EC-1 currently uses “heat-sink” hardware. The additional uncertainty in efficiency related to not accounting for this energy loss is not addressed in this work. However, the importance of these corrections cannot be over estimated. An accurate comparison of hardware or fuels requires this energy to be accounted for as the heat loss is not necessarily equivalent when hardware or fuels are changed. Future work will detail the corrections and the uncertainties associated with them.

The calculation of the theoretical value of the characteristic exhaust velocity is complex, so no attempt to replicate the equations is made here. The CEA code is used with the rocket selection. A finite chamber option is chosen, so the area ratio (between the chamber and nozzle) is an important parameter. The enthalpy (of formation) and chemical equation for the fuel are inputs because RP, the typical fuel of choice, is a blended fuel. Therefore, uncertainties in the heat of combustion and stoichiometric parameters are introduced. The final inputs are the reactant temperature at the inlet, the mixture ratio (oxidizer-to-fuel ratio by weight) and the chamber pressure [12]. Uncertainties in these six parameters are each given their own subsections as well.

The final section combines the above information to get an overall, combined uncertainty in c*-efficiency for the EC-1 engine. From (1) this combined uncertainty is calculated as

$$u(\eta_{c*}) = \eta_{c*}\sqrt{\frac{u^2(c^*_{theo})}{c^*_{theo}} + \frac{u^2(c^*_{actual})}{c^*_{actual}}} \tag{3}$$

The uncertainty in c^*_{meas} is, in turn, calculated (per (2))

$$u(c^*_{meas}) = c^*_{meas}\sqrt{\frac{u^2(P_c)}{P_c^2} + \frac{u^2(A_t)}{A_t^2} + \frac{u^2(\dot{m}_{total})}{\dot{m}_{total}^2}} \quad (4)$$

and the uncertainty in c^*_{theo} is

$$u(c^*_{theo}) = \sqrt{\begin{matrix} s_{MR}^2 u^2(MR) + s_{AR}^2 u^2(AR) + s_x^2 u^2(x) + s_x^2 u^2(y) \\ +s_{\Delta H}^2 u^2\left(\Delta H_{f,CxHy}\right) + s_{\mathrm{Pc}}^2 u^2(P_c) + s_{\mathrm{T_R}}^2 u^2(T_R) \end{matrix}} \quad (5)$$

where *s* are sensitivity coefficients determined directly from the CEA code. Details on their determination are given in a separate subsection at the end of this paper.

SOURCES OF UNCERTAINTY

These are broken out into their own subsections below. This title is included only to maintain consistency throughout the document.

PRESSURE

BASIC PROCEDURE OVERVIEW

Pressures are measured using diaphragm transducers. They are calibrated in-situ (with the wires, signal processing, data acquisition and display systems) using a Ruska model 7310 triple-scaled pressure controller. Several transducers, all having the same range, are attached to a manifold which is brought to and held at a stable pressure. Ten seconds of data is recorded at 1 kHz resulting in 10,000 measures of voltage. (Voltage is measured by setting the engineering unit conversion to 1 and the offset to 0 in the Pacific Instruments PI-6000 signal processing unit; after calibration, the calculated fit and offset are supplied so that pressure is recorded instead of voltage.) Because the temperature and pressure are held steady throughout the 10 seconds, each measurement is assumed to be independent and the data, therefore, represent 10,000 independent measurements for statistical analysis. Figure 2 is an example of the 10,000 data points recorded with one transducer for one pressure. Ten different pressure levels evenly spaced over the range of the transducer are selected. Measurements are made at each pressure moving from atmospheric (psig=0) to the maximum of the pressure transducer and then from the maximum back to atmospheric. This cycle is repeated once more but at only five levels—every other point from the ten original levels. The transducers are then placed back into the engine plumbing and another set of transducers is calibrated until all transducers in the system have been calibrated.

The zero point of the calibration is set to be atmospheric pressure; i.e., in the absence of pressure supplied by the pressure controller, the reading will be the zero point. Atmospheric pressure is measured by an MKS Baratron 722B manometer mounted in the experimental cell and recorded during each calibration and during each test. The manufacturer lists its range as up to 1000 Torr—just over 19 psi or about 1.3 atm. The manometer is calibrated yearly by the AF metrology laboratory following the manufacturer's recommended procedure. This process provides NIST traceability.

The Ruska pressure controller is calibrated every six months to the manufacturer's tolerances. This calibration is performed by an outside laboratory that provides a certification traceable back to a NIST standard. Calibrations

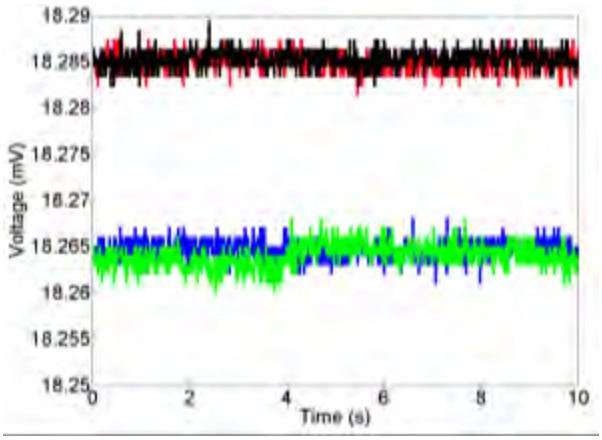

Figure 2. An example of the transducer data recorded as part of the Type A analysis during calibration. During the upward and downward cycling, five of the pressures are recorded four times; all four of the 1800 psi calibration points are shown.

of the EC-1 system transducers are conducted before and after a test series. For a test series involving multiple fuels or hardware components, the calibration is performed before and after each change of fuel and hardware. Results from calibration to calibration are compared to assess the calibration time frame (provide in-tolerance probability [2]) and to provide additional information on the uncertainty between the calibration operations.

Prior to each day of testing, the data acquisition system (Pacific Instruments PI-6000) is calibrated using its voltage calibration source (Krohn-Hite 522 or 526, depending on availability). These calibrations are done internally within the Pacific Instruments (PI) software. Before each run the PI system adjusts the zero point to be consistent with the current atmospheric pressure; transducers are open to the atmosphere during this process. Because the transducers are calibrated in-situ, the uncertainties associated with these procedures are considered to be captured in the statistical assessment discussed in the first paragraph of this section and the atmospheric pressure analysis.

MATHEMATICAL MODEL

In the strain-gauge type transducers being used, the pressure is linearly proportional to the voltage. As mentioned above, the zero point is taken to be atmospheric pressure, so this pressure must be added back to get to absolute pressure

$$P_{supply} = P_{atm} + C_1 V + C_0 \tag{6}$$

where C_1 is the proportionality constant (slope) determined from the calibration. The linear fit is determined using the weighted least squares method outlined in Mathioulakis and Belssiotis [13]. Prior to the recent upgrades, a basic least squares fitting technique was used. While this procedure is sufficient for generating the constant in (6), it does not include the full uncertainties in measurements into the fit nor does it provide information on the uncertainty in the fit parameters. The chosen weighted squares method specifically considers the uncertainty in each variable (here, P_{supply} and V). Many other methods assume that the uncertainties in the two parameters are equal or that the uncertainty in one is zero. Neither of these assumptions applies here or in the majority of other measurements.

The uncertainty and measurement of the atmospheric and supplied pressures are independent of the slope and voltage measured during calibration; it will be assumed that the only cross-correlation is entirely taken into account through the curve-fitting procedure for determining the uncertainty in the line fit constants [13]. The combined uncertainty in the pressure is then

$$u(P) = \sqrt{C_1^2 u^2(V) + V^2 u^2(C_1) + u^2(C_0) + u^2(P_{atm}) + 2V cov(C_0, C_1)} \tag{7}$$

An additional uncertainty term $u(P_{supply})$, the uncertainty associated with the pressure controller's set point, also comes into play. It is supplied (along with the uncertainty in measured voltage) during the weighted least squares fit and impacts the uncertainties in C_0 and C_1.

SOURCES OF UNCERTAINTY

Each of the uncertainty terms within the combined uncertainty of the pressure may be broken down into several specific uncertainties. (The model for these individual component uncertainties is additive in quadrature [2, 3].) The specific and combined uncertainties are given in Table 2 and the breakdown of each component's contribution is illustrated in pie, Fig. 5.

The voltage uncertainty, $u(V)$, is composed of the resolution of the system, changes in the temperature (environment and fluid being measured), the supplied power to the transducers and repeatability (i.e., "random error"). The resolution on the DAQ system is 16-bit, but the output values are rounded to the nearest 0.01 volt (or psi during pressure measurements). This resolution is also larger than the sensitivity of the transducers. This value is chosen because it is small enough that the uncertainty in resolution is negligible. (Note that while pressures are recorded to 0.01 psi resolution, they would not be reported to that level of resolution because of the substantially larger uncertainty.)

These transducers also have uncertainties associated with the temperature of the diaphragm (and Wheatstone bridge). Currently, the transducers in EC-1 are not temperature compensated. The

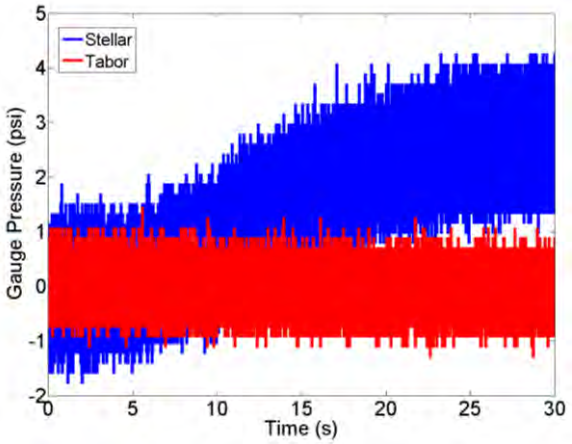

Figure 3. The measured pressure changes noticeable from the warm of a hand on the Stellar ST1500 transducer body. The Tabor transducer does not have the same rise. Both transducers are regulated, not the unamplified currently in use.

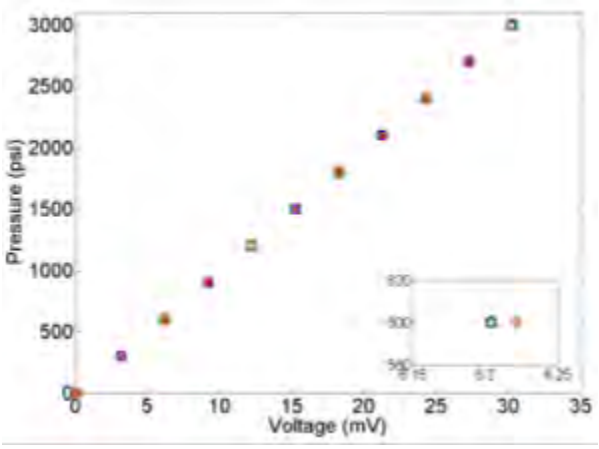

Figure 4. A set of data from the calibration of a single Tabor transducer. The colors/symbols represent the different cycles, and the inset illustrates the hysteresis of the transducer.

uncertainty associated with temperature given in Table 2 is the manufacturer's given uncertainty. It should be noted that EC-1 had used transducers (Stellar model ST1500, generally with a 3000 psi range) which were temperature compensated and rated as stable over a temperature range of -65 to 250°F. However, wrapping one's hand around the transducer for a few seconds would cause a noticeable shift in measured pressure (Fig. 3). While the current transducers, Tabor model 2211, also exhibit some shift, but this is expected as they are not internally temperature compensated. A correction factor must be calculated during calibration to account for temperature shifts. Future plans call for determining these factors by conducting some calibrations in an oven. Two types of heated calibrations will be performed. In one, the pressurized block will be heated in a Tenney TJR while the transducer body remains outside, simulating the exposure of the diaphragm to high temperature gas. In the other type of heated calibration, the transducer itself will be heated along with the pressurized manifold. With this procedure, changes in test-cell temperature can be simulated. This second technique has been suggested in the past for calibrations for rocket engines [14]. The temperature of the diaphragm is recorded by an internal RTD in the Tabor transducers. (This RTD is powered by a Pacific Instruments 6018-3 card and recorded on the DAQ system.)

Most transducers claim to be independent of the supplied power. However, experience with chopping power supplies (typically called a regulator) indicated that this independence was not achieved in EC-1 with amplified transducers (several manufacturers were tested); these would feed back to one-another and the output of all transducers would oscillate in phase. As a result, the amplified transducers relying on chopping power supplies were removed and unamplified transducers being powered by the data acquisition system (via a Pacific Instruments 6032-EM card) are being used. Oscilloscope traces of the output indicate there is no longer oscillatory behavior. Furthermore, the transducers are now isolated into groups of no more than four on a single supply card, so any feedback is limited to a smaller number of transducers.

Diaphragm transducers always have some level of hysteresis due to the flexing and relaxing of the metal diaphragm. The two upward-downward cycles during calibration enable the determination of an uncertainty associated with this effect. It is essential to carry out a series of upward and downward cycles in order to evaluate this uncertainty. The four measurements at each point all independently included in the linear fit (i.e., the points are not averaged together prior to fitting the line). Figure 4 illustrates the hysteresis in a single transducer by showing the voltage values for all four cycles. The hysteresis value itself is not contained in the uncertainty analysis, but its value impacts the uncertainties in the constants calculated from the calibration.

An additional, unexpected effect that has been observed in EC-1 is a change in the calibration curve due to tightening or loosening the fitting in the bottom of the transducer. This change only occurs when the transducer has a female opening and can be mitigated by taking care to never adjust the connection into the transducer following calibration. However, EC-1 had moved to male connection on the transducer bodies and is now moving to the Tabor 2211 transducers which do not suffer from this issue. Subsequent to discovering the issue, similar problems were found documented in an earlier examination of uncertainty in monopropellant rocket engines [14].

Other sources of uncertainty exist in the voltage measurements; these are lumped together into the heading “repeatability” and are assessed using Type A analysis (i.e statistics) from the 10,000 repeated measurements at each point [2, 3]. Again, a typical set of data over the 10 second recording window is shown as Fig. 2.

A linear fit of the average voltage, averaged over the 10,000 data points at each pressure, versus the supplied pressure is calculated using a weighted least squares method [13]. Thirty total points are included in the fit due to the cycling used to elucidate hysteresis effects. The fitting method considers the different specific uncertainties in the voltage and supplied pressure to generate the uncertainty in the coefficients; the technique also generates a covariance. (The uncertainty in supplied pressure is discussed below.) The final coefficients are compared to prior calibrations and their associated uncertainties. If indicated by this comparison, the uncertainty in the measurements made between calibrations is increased from that given by the first calibration. The comparison is also used to assess the calibration period [2]; if large deviations were observed, the calibration period would be shortened.

The bulk of the atmospheric pressure uncertainty is taken from the manufacturer’s specifications. The manometer is calibrated biyearly to the manufacturer’s specifications by the local AF metrology laboratory. The range and uncertainty of the Ruska pressure controller prevents in-situ calibration. The value is recorded on the data acquisition system during calibration, but the repeatability uncertainty is included in the manufacturer’s specifications combined with the nonlinearity and hysteresis, so a Type A analysis has not been performed for this instrument. It is given as 0.5% of the reading for an ambient temperature range of 0 to 50°C. EC-1 operates within this temperature range with typical atmospheric pressures from 13 to 13.5 psi. Additionally, there is an uncertainty associated with the recorded resolution. The manometer is not temperature controlled; the manufacturer gives the uncertainty in temperature coefficients. These are not currently included because the manufacturer has not yet provided clarification as to their application.

The pressure controller has a manufacturer stated specific uncertainty determined from an error analysis in a manner predating the GUM guidelines. It will be assumed here that these are true uncertainties given without confidence bands; this assumption is more conservative than its opposite. An overall accuracy is given as well as a stability and resolution. The manufacturer’s total uncertain, given in Table 2, is a combination of the above specific uncertainties. A one year recalibration interval is recommended; however, a 6 month calibration period is employed due to AF instructions. From an examination of newer models, it is likely that these uncertainties only apply to pressures from 5 to 100% of full scale, although no specific mention of this is given in the literature for the 7310 model. The instrument in use in EC-1 is triple-scaled having independent full scales of 6000 psi, 4000 psi and 2000 psi. The use of a triple-scaled controller is essential to maintain low uncertainties over wide the range of pressures measured in EC-1. This point highlights the need for careful selection of instruments, which should always be chosen to match the expected measurement value. For example, consider a hypothetical manufacturer’s uncertainty in the transducer used to measure the atmospheric pressure. Assume this is given as 0.1% of full scale—a typical value for many of the transducers used in EC-1. Using the same 0-3000 psi transducer range to measure the chamber pressure and the atmospheric pressure would result in an atmospheric pressure reading of 13 +/- 3 psi; alternately, choosing a transducer with a 0-15 psi range and the same uncertainty percentage to make the same measurement would yield 13.400 +/- 0.015 psi.

COMBINED UNCERTAINTY

Using (7) and the uncertainty values given in Table 2, the combined uncertainty is between 0.28 to 0.45 psi for the range of pressures from 300 to 3000 psi. Note that these values are for a single,

Parameter	Source of Uncertainty	Uncertainty Value	Distribution of Uncertainty	Degrees of Freedom
Voltage	Temperature	Left to future work		
Voltage	Type A	0.0011 mV (avg)	Normal	9,999
Supply Pressure	Manufacturer's Specifications	0.014% Full Scale		
Supply Pressure	Resolution	0.001% Full Scale	Uniform	Infinite
Supply Pressure	Total	0.0142% Full Scale		
C_0	Total	-19.085		
C_1	Total	99.618		
$Cov(C_0,C_1)$	Total	-0.0022		
Atmospheric Pressure	Manufacturer's Specifications	0.5% Reading		
Atmospheric Pressure	Resolution	0.005 psi	Uniform	Infinite
Atmospheric Pressure	Total	$0.005\sqrt{1+(\text{Reading})^2}$		
Pressure	Total	0.28 to 0.45 psi (0.092 to 0.014%)		

Table 2. The uncertainty in the pressure measurements. FS is full-scale and is either 2000, 4000 or 6000 psi (the smallest usable) depending on the transducer range (4000 psi for the example for which the totals are calculated). The total value is likely low because temperature compensation and its related uncertainties have been neglected here pending additional analysis. The Type A analysis and curve fits were performed for a single, 3000 psi Tabor transducer. C_0=-19.0792 and C_1=99.6177 for pressures in psi and voltages in mV. The totals are for pressures from 300 to 3000 psi.

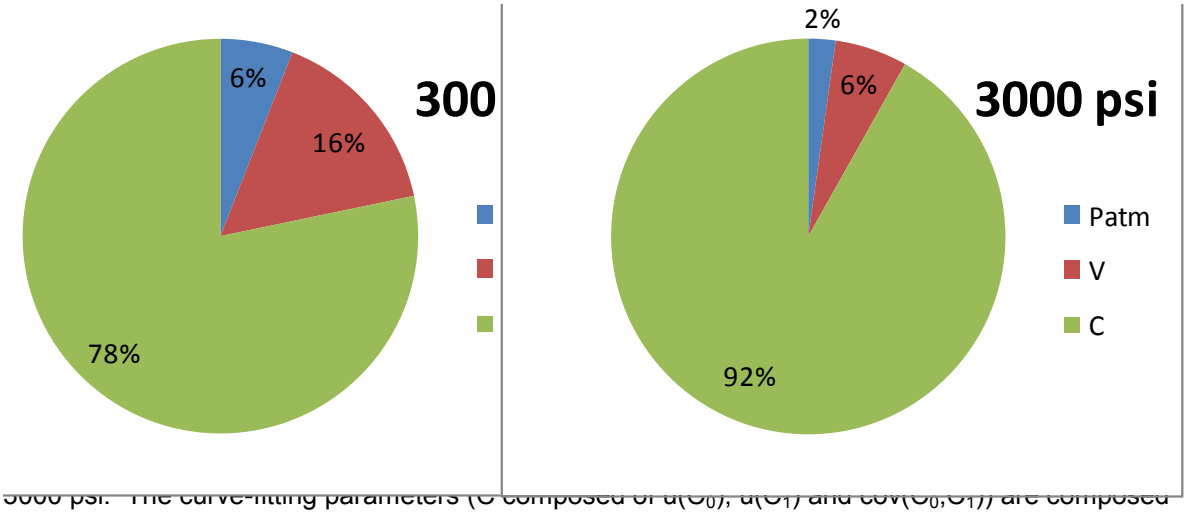

3000 psi. The curve-fitting parameters (C composed of $u(C_0)$, $u(C_1)$ and $cov(C_0,C_1)$) are composed of the uncertainty in supply pressure, voltage and the spread of the data.

randomly selected Tabor transducer. The uncertainty prior to going to the high-accuracy, not temperature compensated, unamplified duties was substantially larger. A randomly chosen previously used transducer had an uncertainty of 9.03 to 9.04 psi for the same pressure range.

The largest contributor to the uncertainty is the curve-fit parameters (for both the current transducers and the older transducers). Prior to the new transducer selection, the spread of the data, i.e. the nonlinearity and hysteresis, and uncertainty in the voltage dominated the uncertainty in fit parameters (and combined uncertainty) accounting for over 99% of the value. Now, while the curve fit parameter uncertainties still dominate, the uncertainty is driven as much by the uncertainty in supplied pressure as

by the uncertainty in the value returned by the transducer. Careful selection and validation of tranducer's capabilities are critical for keeping the pressure uncertainty low.

BEST PRACTICES AND ADDITIONAL CONCERNS

As in all the following sections, the above analysis has only included the uncertainty in the diagnostic system itself. There is always additional concern and uncertainty related to whether or not the diagnostic is measuring the parameter of interest. For example, chamber pressure is generally assumed to be a single value, but there can be pressure loss along the length of the chamber, so it is important to design and instrument enough to capture this change if it exists [7]. Additionally, the pressure measured in the chamber is a static pressure, but the pressure which should be included in the c^* calculations is the total pressure. The velocity of the chamber must be known to correct the pressure, and that introduces additional uncertainty. In the EC-1 facility, pressure is typically measured in two locations, near the middle of the chamber and near the nozzle. When testing is done with the 2" internal diameter engine sections, the pressure loss along the engine is negligible; with the 1" internal diameter sections, the loss is measurable. However, at this time EC-1 uses only the measurement from the near nozzle transducer in its calculations. No correction to stagnation pressure is attempted despite the relatively large area ratios at which the engine operates. Future plans call for introducing these corrections.

The transducers are located on long leads so that they are not exposed to the high gas temperatures or soot which could impact measurements and decrease sensor lifetime. Future upgrades include adding a very low velocity Helium purge (aka, snubbing) to the transducer lines. This upgrade should improve transducer lifetime, mitigate temperature changes at the diaphragm and, due to the low density of Helium, improve the response time of the transducers. Currently, however, the instruments are inspected for signs of wear and build-up of soot prior to calibration. The calibrations and during-test performance are also monitored for sudden changes and other signs indicating the end of transducer lifetime.

Several uncertainties have been reduced through experimental set-up and selection. The following are recommendations of best practices for pressure measurements in small-scale engines.

- Perform calibrations routinely
  - Compare with prior calibrations and uncertainty to determine if cycle is too long or short
  - Calibrations should be used to "validate" the uncertainty promised by the manufacturer and, therefore, assess if accuracy can be lowered by choosing different transducers
  - Calibrations should be performed in-situ (this gives repeatability values without the need to calibrate each system component)
- Match the transducer range to the expected values
- To elucidate hysteresis, perform multiple cycles in alternating directions during calibration
- Do not rely on internal temperature compensation, verify as possible. In EC-1's experience, heating the transducer body using typical body warmth may be sufficient to show that the temperature compensation is not reliable.
- Be aware that changes in fitting tightness into a female transducer body may impact calibrations. Use male bodies if possible, take extra care to not change the fitting tightness into the transducer, and verify there are no changes if the fitting is altered
- Record atmospheric pressure during the test
- Take pressure measurements at multiple locations along the length of the engine and correct for velocities and pressure losses.
- Use a weighted least squares curve fitting which does not assume negligible uncertainties or equal uncertainties in both parameters to calculate the uncertainty in fit parameters and to include uncertainties in measurements in the fit.

- Protect the transducers from soot and high temperatures. Ideally, this is accomplished through snubbing with a low-density gas (to increase response time), but it can also be done with reasonable line lengths.
- Ensure transducer output is independent of the power supply by checking the output of at least one transducer with an oscilloscope. Checks should be performed with all system transducers inserted into the system.

TEMPERATURE

BASIC PROCEDURE OVERVIEW

A thermocouple simulator is used to calibrate the temperature measuring system without the thermocouples. An Ectron 1140A simulator uses programmed NIST tables to convert an entered temperature to the emf which would be produced by a selected type of thermocouple at that temperature. The signal processing/data acquisition system reads this emf and, again using programmed NIST tables, converts the measured emf to a temperature. The temperature is recorded at 1 kHz for ten seconds. There is no reason to believe the system has any hysteresis (and this is easily verified), so a single, upward cycle is used. All types of thermocouples are calibrated at 20°C increments over the range of the thermocouple. The measured temperatures and the ranges during calibration are absolute values, not values in reference to a junction temperature; however, the signal processing/DAQ unit could automatically compensate for any junction temperature.

EC-1 contains two-hundred hot-box compensated thermocouple channels. It is impractical to calibrate all channels, particularly on a recurring basis. Given that all channels are tied to the same hot-junction box, have similar wire lengths and are, in general, identical to one another, full calibration of all channels is also considered unnecessary. Instead, five randomly chosen channels of each thermocouple type are calibrated yearly. These five channels are chosen from those currently in use. Other channels are verified at two points—room temperature and the triple point of water prior to being placed in service. The thermocouple simulator is calibrated yearly to manufacturer's specifications by Edwards AFB's calibration laboratory. (The specifications for the calibration show how that process is NIST traceable.)

Thermocouples themselves are not calibrated in-house. Select thermocouples from each shipment are verified. Again, this verification is conducted through measurements of room temperature and the triple point of water using the Ectron 1140A's capabilities. The reason for this procedure is the sheer volume of thermocouples handled in a given year. An assumption has been made that thermocouples from the same manufacturing lot will have similar uncertainties. No attempt has been made to verify this claim at the EC-1 facility.

Prior to each experimental test, the temperatures on all channels in use are confirmed. If the measurements are outside of expected values or a single thermocouple reading is out of line with nearby instruments, the cause of the discrepancy is investigated and fixed, sometimes necessitating the replacement of thermocouples, before testing continues.

MATHEMATICAL MODEL

The set (aka, simulated) and recorded temperatures are compared to one-another and a linear curve is fit to the results

$$T_{supply} = C_0 + C_1 T_{record} \tag{8}$$

If the system was perfectly calibrated C_0 would be 0 and C_1 would be 1. In addition to the uncertainties in the parameters of (8), there are uncertainties associated with the value output on the simulator and by the thermocouple itself. Also, EC-1 uses a hot junction box (discussed in more detail below), so the uncertainty in the junction temperature must be considered. The measured temperature is really the difference between the junction box temperature and the temperature of the probe, so this uncertainty combines additively. Combining all of these uncertainties gives

$$u(T) = \sqrt{\begin{matrix} C_1^2 u^2(T_{record}) + T_{record}^2 u^2(C_1) + u^2(C_0) + 2T_{record} cov(C_0, C_1) \\ +u^2(T_{jun}) + u^2(T_{tc}) \end{matrix}} \quad (9)$$

As with the pressure, the linear fit is determined using a weighted least squares method [13] which gives the uncertainties in the coefficients as well as their covariance. The uncertainty in the thermocouple, junction temperature and the simulator are independent of each other so no additional covariances exist.

SOURCES OF UNCERTAINTY

The specific uncertainties in (9) can be broken down into several uncertainties. Again, the model for the individual component uncertainties is additive in quadrature. Table 4 and Fig. 7 list the specific and combined uncertainties for type E and K thermocouples. Values are given for these types because they are the most commonly used during testing in EC-1. The main difference in the uncertainty values is in the thermocouple itself and the temperature ranges calibrated: the uncertainties other than those of the thermocouple itself may be considered representative for all types.

The uncertainty in the thermocouples is taken from manufacturer literature. EC-1 uses thermocouples from two manufacturers—Omega and Nanmac. The uncertainties are similar across the two manufacturers (and across other manufacturers). In general, the uncertainties listed by Omega are larger at temperatures near 0°C (32°F) because Omega lists a flat value or a percentage, whichever is larger. The uncertainties for each manufacturer across the three standard types of thermocouples are given in Table 3.

Type	Range	Omega	Nanmac
K	<0°C	2.2°C or 2.0%	2.00%
K	>0°	2.2°C or 0.75%	0.75%
T	<0°	1°C or 1.5%	1.50%
T	0-200°	1°C or 0.75%	1.50%
T	>200°	1°C or 0.75%	1.00%
E	<0°	1.7°C or 1.0%	1.00%
E	0-200°	1.7°C or 0. 5%	1.00%
E	>200°	1.7°C or 0. 5%	0.50%

Table 3. Manufacturer's given uncertainties for different thermocouple types. Where two values are listed, the larger of the two should be used. Values given by both Omega and Nanmac are in °C.

The uncertainty in the measured temperature is a combination of resolution and uncertainties assessed through Type A analysis (repeatability). Several items are included within the Type A assessment such as noise, the effect of wire length, instability in the junction temperature and

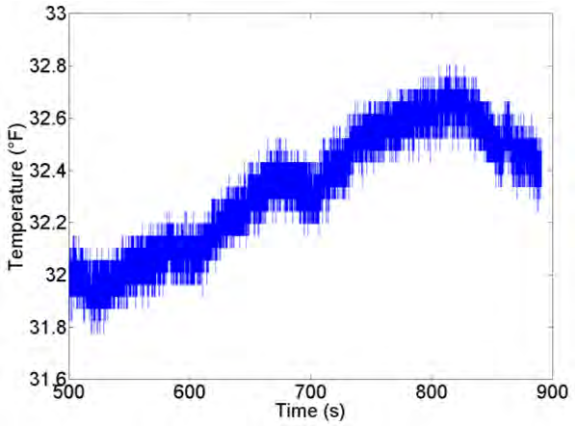

Figure 6. The temperature of the junction box changes slowly over time as seen by the results of measuring an ice-water bath over a long period of time.

Type	Range °F	Accuracy	Total
K	-427 to -319°	0.72°F	0.74°F
K	-319 to -175	0.20	0.27
K	-175 to -67	0.14	0.23
K	-67 to 1832	0.13	0.22
K	Above 1832	0.14	0.23
T	-427 to -400	0.63	0.65
T	-400 to -346	0.45	0.49
T	-346 to -238	0.27	0.32
T	-238 to -40	0.18	0.25
T	14 to 212	0.13	0.22
T	Above 212	0.11	0.22
E	-409 to -319	0.29	0.34
E	-319 to -247	0.16	0.23
E	-247 to -130	0.13	0.22
E	Above -130	0.11	0.22

Table 4. The uncertainty of the Ectron thermocouple simulator.

uncertainties introduced from the DAQ system. The DAQ system is carefully grounded to minimize noise. Long wires increase the resistance of the system; this degrades signal and introduces uncertainty. Thermocouple manufacturers recommend lengths under 100 feet with AWG 20 are larger wire [15]. Thermocouple-grade wire is used up to the junction box, so reducing its length also reduces costs. The junction box used in the facility is located just behind the engine, within a few feet of all measurement ports, to minimize wire length. Furthermore, the signal processor/DAQ system is also located within the experimental cell (in a climate controlled chassis) to reduce wire length following the junction box.

As with the pressure, a weighted least squares method [13] is used for the linear fit. The fit is compared to the ideal—C_0=0, C_1=1—and the uncertainties and covariances are compared with previous calibrations. A substantial increase in uncertainties would be unexpected and would likely indicate a problem with the system. If an increase was found, the uncertainty in measurements made between calibrations would be updated to reflect the higher uncertainty value.

A junction box is critical to maintaining low uncertainty in the EC-1 facility because the engine is not in a climate-controlled environment. Because the experimental cell can get to summer desert temperatures, over 110°F, a cold junction at 32°F is impractical. Instead, a hot junction box is used, which is kept at 150°F. Currently, the junction box temperature is measured by an RTD and recorded during the test. The signal processor adjusts the recorded temperature assuming the junction is at the

Parameter	**Source of Uncertainty**	**Uncertainty Value**	**Distribution of Uncertainty**	**Degrees of Freedom**
Thermocouple	Manufacturer's Specifications	See Table 3		
Recorded Temperature	Resolution	0.005°F	Uniform	Infinite
Recorded Temperature	Random	0.096°F	Normal	9,999
Recorded Temperature	Total	0.096°F		
C_1	Total	0.0380		
C_0	Total	2.2067×10^{-4}		
$Cov(C_0, C_1)$	Total	-6.7506×10^{-6}		
Junction Box Temperature	Resolution	0.005°F	Uniform	Infinite
Junction Box Temperature	Stability	0.03°C		
Junction Box Temperature	RTD measurement	0.01°C		
Junction Box Temperature	Total	0.032°C		
Supplied Temperature	Total*	0.23°C		
Temperature	Total (Type E)	Nanmac 1.00-1.02% (T_{jun}-T_{record}) Omega 1.002°C		
Temperature	Total (Type K)	Nanmac and Omega 2.00% (T_{jun}-T_{record})		

Table 5. The specific uncertainties associated with temperature. The combined uncertainty is given for type E thermocouples between 40 and 100°F; this thermocouple and range would be typical for the propellant feed system. Combined uncertainty is also given for a type K thermocouple in the range of 300-500°F<?>--a thermocouple and range typical of the engine. The linear fit is performed in °C and the constants are C_0=-0.0098 and C_1=0.9999 for the uncertainties given here, those from a calibration of a random Type E channel of the system.

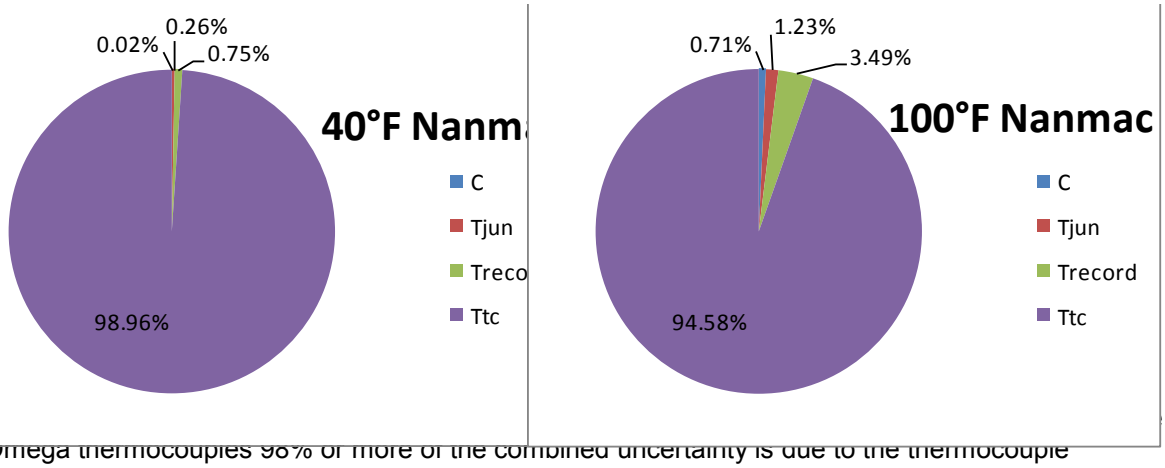

Omega thermocouples 98% or more of the combined uncertainty is due to the thermocouple uncertainty over all operating conditions and types.

preset value of 150°F. The recorded RTD temperature is used to correct for any offset or change in junction box temperature away from the expect 150°F value. The variation in the junction temperature with time is accounted for by in-situ variation (i.e., the Type A analysis discussed above). However, the uncertainty in the raw value must be considered since it is used as a correction factor. An example of the slow change in time is shown as Fig. 6. According to Isotech, the stability of the system is 0.03°C. The junction box temperature is recorded from an RTD with an accuracy of 0.01°C and a resolution of 0.01°F. The RTD is calibrated using ITS-90 standards.

The Ectron model 1140A thermocouple simulator is designed specifically for calibration purposes. It can both precisely simulate thermocouple emf and precisely measure the emf generated by a thermocouple (including simulating the junction temperature). It has a low output impedance, less than 0.05 Ohms, and a high input impedance, 10MΩ, to minimize noise in the system associated with the supply of a voltage. The accuracies, reproduced below (Table 4) from the Ectron's data sheet, include conformity, noise and stability. They are applicable to the 6-month calibration period employed by EC-1. As with the thermocouple uncertainties, it should be remembered that the ranges given here refer to differences from the hot junction temperature of 150°F, i.e. they are not absolute temperatures, due to the set-up of the EC-1 facility. The temperature supplied by the thermocouple simulator does not appear in (9) explicitly but effects the curve fit parameters and their uncertainties as shown in (8).

COMBINED UNCERTAINTY

Figure 8. A typical temperature trace form the <locations?> during an engine firing in EC-1.

The values in Table 3 combined with (9) give a combined uncertainty of 1% of the recorded value (in °C) if using Nanmac type E thermocouples for typical fuel inlet temperatures (40 to 100°F). For the same conditions, the Omega thermocouples would have a combined uncertainty of 1.002°C. This uncertainty is better than what could be achieved with Type K thermocouples in that range (those would be on the order of 2% or 2.2°C for Nanmac or Omega, respectively). For engine temperatures type K thermocouples would be used with an expected range of <300 to 500°C>. The combined uncertainties in this situation are 2.00% of the recorded temperature (in °C) or between 2.201 and 3.890°C (2.00% over 350°C) for the Nanmac or Omega thermocouples, respectively.

The largest contributor the uncertainty is the uncertainty in the thermocouple itself. While this uncertainty could be reduced by moving from thermocouples to other temperature measurement devices such as RTDs, the response time would suffer. A typical complete test cycle is less than 10 seconds and temperature changes over milliseconds can be important and should be captured; at times, particularly when valves open, these temperature changes can be very steep. RTDs do not allow an adequate level of temporal resolution for these step changes. Figure 8 shows some typical temperature traces from a single engine firing indicating the type of rapid changes which must be captured. Some of these changes can be ameliorated by ensuring valves are downstream of orifice flow meters. Another choice which can improve the combined uncertainty is to use a thermocouple type with a lower uncertainty over the range of interest. Type E thermocouples are used for the fuel measurements for this reason. It may be possible to further reduce uncertainty by calibrating the thermocouple and using the specific uncertainties of the thermocouple itself; however, any reduction would indicate a thermocouple which was better than expected by the manufacturer, so much gain using this approach would be unlikely. The calibration and usable range could be set to a smaller range allowing the gain on the DAQ to be increased. While this might decrease the uncertainty in the recorded temperature and the spread of data slightly, channels would need to be labeled and dedicated to certain parts of the engine and an anomaly might exceed the measurable range of the DAQ and, therefore, not be recorded. Given the extremely small impact this change would have on uncertainty, Pacific Instruments recommended gains for thermocouple types are used instead of tailoring the gain to the specific expected range.

BEST PRACTICES AND ADDITIONAL CONCERNS

Again, the analysis above is for the measuring system only. Additional uncertainties exist in relation to the probe's ability to measure the temperature of interest. Wall temperatures and heat fluxes can be measured with embedded thermocouples or eroding thermocouples. An assessment of uncertainties associated with the embedded process in EC-1 can be found in [16]. Thermocouples used to measure propellant temperatures are inserted approximately to the centerline of the supply lines (1/2" supply for liquid fuel, 1' for gaseous oxidizer); location is confirmed by eye. It is assumed that they measure the average, bulk temperature of the propellant or oxidizer with no correction. To help ensure this is the case, velocities at the measurement location should be low (more details on this are given in the mass flow rate section) and the thermocouple should not be in the boundary layer. Additionally, care must be taken to avoid adiabatic compression when valves open. Such a state causes a sudden change in temperature and the thermocouple's relaxation times do not allow it to recover over the several-second period of testing. The compression problem can be particularly troublesome upstream of orifice flow control devices because it is easy to cause compression and because the upstream temperature is an important measure for accurately determining the flow rate (see the section on the mass flow rate of the gas).

The following are a list of recommendations and best practices for minimizing uncertainty in temperature measurements

- Use a controlled junction temperature
  - Record this temperature during the test and correct for any changes from the assume value
- Wire length should be kept to a practical minimum with the junction box located a near as feasible to the measurement location
- Thermocouple grade extension wire is recommended to the junction box
- Verify or calibrate all channels prior to use
- Take care in component placement to avoid adiabatic compression
- Uncertainty of the thermocouple itself is the largest contributor to overall
- Choose high-accuracy thermocouple types for measurements where lowering uncertainty is of prime importance.

NOZZLE AREA

BASIC PROCEDURE OVERVIEW

Nozzle area is not measured directly. Instead, the nozzle diameter is measured with the use of pin gauges. Diameter is measured following every test. Several pin gauges near the expected diameter are taken to the nozzle. Each is inserted to ascertain which is the largest that will fit. Care is taken to insert the gauge straight into the nozzle, with axes aligned. At times, more than one user will make the same measurement; however, the number of measurements remains too low for statistical analysis. No attempts are made to ensure consistent temperature of the pin gauge or nozzle prior to and during measurement. The pin gauges are stored in a controlled environment, but may be in the uncontrolled test cell or the user's hand for a variable amount of time. The nozzle is water cooled and should rapidly reach the temperature of the water following the test; however, the water is stored outside and is not, itself, a controlled temperature. Prior and following use, the gauges are checked for signs of wear.

MATHEMATICAL MODEL

The nozzle throat is assumed to be circular so that its area is

$$A_t = \frac{\pi}{4} D_t^2 \tag{10}$$

This simple formula results in an area uncertainty of

$$u(A_t) = A_t \frac{u(D_t)}{D_t} \tag{11}$$

As with the temperature and pressure, however, the uncertainty of the diameter is itself composed of several individual uncertainties. These are considered to be independent and are listed in Table 6 and Fig. 9.

SOURCES OF UNCERTAINTY

Pin gauges are available in increments of 0.0005 inches in EC-1. Half of this, then, is the resolution uncertainty for the diameter measurement. Experience with the gauges indicates that the user-to-user variation is within a single increment of the pins. All those taking measurements are trained to take care that the gauge is inserted straight and flat into the nozzle throat and to not force the gauge into the throat. More than one fit is attempted. As a result, the bias introduced by the individual is considered to be equivalent to the resolution available on the gauges. A main reason for using the pin gauges is that measurements with them are very repeatable. Previously, nozzle diameter was measured using a bore micrometer. User-to-user variation was seen to be 0.005 inches or greater—an order of magnitude larger uncertainty than that obtained using the pin gauges.

The pins in use are Black Guard gauges manufactured by Vermont Gage and of the Class ZZ variety. Per ANSI/ASME B89.1.5, Class ZZ gauges are accurate to 0.0002 inches from 0.01 to 0.825 inches [17]. The typical throat diameter in EC-1 is between 0.45 and 0.65, so measurements are within the cited range. (In EC-1 gauges are available up to 1 inch; over 0.825 inches these have an accuracy of 0.00024 inches.) Black Guard gauges were purchased due to their black oxide coating. Not only does this coating protect from corrosion, but it also gives an indication of wear. According to the manufacturer, the black finish penetrates to between 0.00004 and 0.00006 inches, so no signs of wear indicate the accuracy of the gauge due to wear are within those bounds (and recalibration is not necessary). The ANSI/ASME standard and thes documentation from Vermont Gage provide NIST traceability.

A worst-case uncertainty due to uncontrolled temperature will be considered. Vermont Gage indicates that the gauges are calibrated at 68°F. For a worst case, assume that the gauge has adjusted to the outdoor environment at 110°F (a hot summer in the desert). The coefficient of thermal expansion for AISI 52100 steel is given as 6.95x10-6/°F [18]. Practically, the gauges would not be in the outdoor environment long enough to reach 110°F since they only remain outside long enough to make the

Parameter	Source of Uncertainty	Uncertainty Value	Distribution of Uncertainty	Degrees of Freedom
Diameter	Resolution	2.5×10^{-4} inch	Uniform	Infinite
Diameter	User Error	2.5×10^{-4} inch		
Diameter	Gauge Manufacturing	2.0×10^{-4} inch	Normal	Infinite
Diameter	Potential Wear	4 to 6 $\times 10^{-5}$ inch	Uniform	Infinite
Diameter	Temperature Gauge	$6.95 \times 10^{-6} * \Delta T D_t$		
Diameter	Total	$4.31\text{-}4.52 \times 10^{-4}$ inch		
Area	Total	$1.52\text{-}2.31 \times 10^{-4}$ inch^2 (0.10 to 0.07% of A_t)		

Table 6. The breakdown of uncertainties in nozzle throat area. The total values assume throat diameters from 0.45 to 0.65 inches (the typical range in EC-1), a change in temperature of the gauge to 110°F, and a maximum wear at 6×10^{-5} inches.

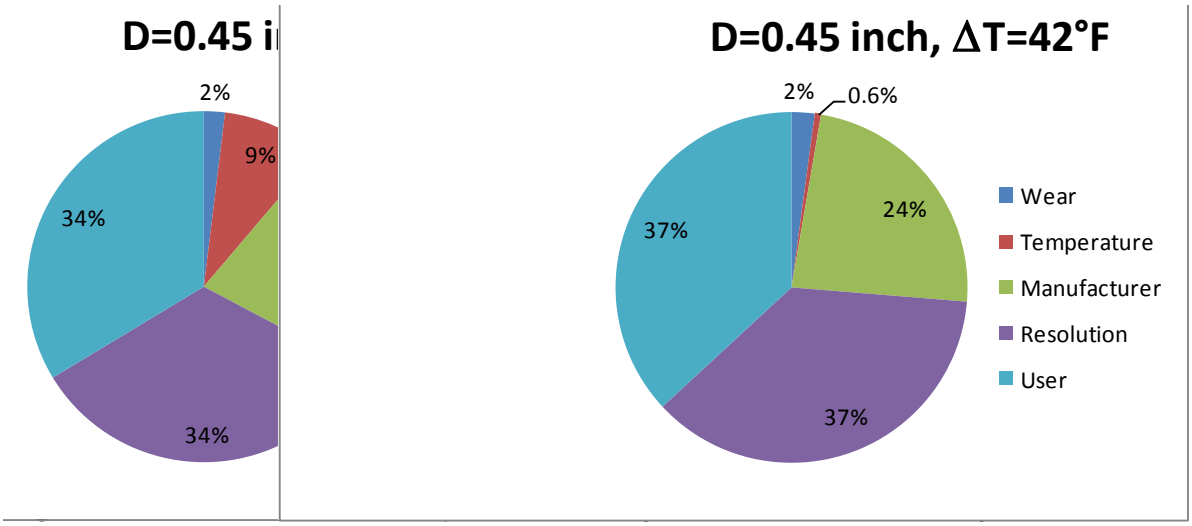

The left figure shows the contributions if the gauge may be heated to 110°F; the right figure shows the contributions if the gauge temperature is known to remain under 78°F.

measurement. Because the time is inconsistent and no effort is spent on trying to maintain or measure the gauge temperature, it seems prudent to use this worst-case value, however. Note that with these assumptions the uncertainty due to temperature changes is not negligible. However, if the change in temperature is assumed to be a more modest (and realistic) 10°F, then its contribution to uncertainty is similar to the wear values.

COMBINED UNCERTAINTY

Table 6 and Fig. 9 give the breakdown for the specific uncertainties which are combined in quadrature to get the combined uncertainty in diameter. For a 0.45 inch throat diameter, the combined uncertainty in area is 1.52×10^{-4} inches or 0.10% of the total throat area. For a 0.65 inch diameter the area uncertainty is 2.31×10^{-4} inches or 0.07% of the total throat area. Both these numbers assume the wear uncertainty at it higher number and a worst-case temperature uncertainty of heating the gauge to 110°F.

The resolution and user bias, which is strongly related to the resolution in this case, dominate the uncertainty. This resolution is not easily changed based on availability in the marketplace. Small gains could be made by moving to Class Z gauges, whose manufacturing tolerances must be half of those for the Class ZZ [17]. However, only a reduction of 7-8.5% in area uncertainty could be made with this change. 4.5 to 8.5% gains could be made by controlling the gauge temperature so that typical changes are within 10°F (with largest improvements being related to the largest diameter gauges. Such modest

reductions are not worth the additional cost to implement. However, following the analysis, additional care is taken to limit the outside exposure and time-in-hand to better reduce temperature changes (the change in temperature remains unmeasured, however).

BEST PRACTICES AND ADDITIONAL CONCERNS

In addition to the instrument uncertainty in measurement, there are two additional effects to be considered wherein the measured value may depart from the intended value. First, the throat diameter is measured following a test, it is not measured during a test. The correct throat area to use in the c^* calculation is that at the time the pressure is measured. The throat may expand due to thermal expansion or crush due to the pressure of the cooling water. An early nozzle design had problems where the throat was being successive crushed over the course of several tests until it reached a steady value. This was measurable after the test, but the size during the test was unknown, so the uncertainty was augmented by (at a minimum) the change in size from before to after the test. Currently, there is typically no measurable change in throat diameter from test to test. It is believed that departures in size due during testing are minimal, but this assertion cannot be verified.

The final uncertainty is the possibility that the throat is not round. The pin gauges will, obviously, measure the minimum diameter in this situation. Some check of circularity can be made by lighting the nozzle behind the pin gauge and checking to see where light escapes, but this technique does not give quantitative values. To date no measures of circularity have been carried out in EC-1. It is known that prior nozzle throats would become egg-shaped over time due to nonuniform cooling. Changes in the nozzle design and water cooling have improved, and the throat is no longer noticeably out of round. As with the changes during firing, it is assumed that this uncertainty has been minimized through nozzle cooling design, but it cannot be verified that the throat remains circular throughout the test.

To minimize uncertainty the following practices are recommended

- Measure the throat area following every run
- If deviations in circularity or size are observed, the nozzle should be replaced or redesigned and the test repeated.
- If changes are measured, the uncertainty for that test must be augmented by the difference in measurement
- The use of pin gauges versus a bore micrometer is recommended to reduce repeatability and user bias
- Pin gauges should have a finish wherein wear is evident or be calibrated regularly
- To fully minimize uncertainty, efforts should be taken to control the temperature of the pin gauges
- Temperature variations under 10°F are sufficient to reduce the contribution of this uncertainty to ~2% or less of the total uncertainty over the typical range of nozzle sizes
- Careful design and analysis of the nozzle should be conducted to increase the likelihood that it maintains its size and circularity during testing

DENSITY

BASIC PROCEDURE OVERVIEW

Densities are needed to calculate the mass flow rate of the fuel. Because blended fuels are typically used in EC-1, densities may change when the batch of fuel changes. Densities are determined following the ASTM D4052 method [19]. This method uses the change in oscillation period due to the addition of a sample to determine the density. It requires initial calibration using air and water to obtain instrument constants. Calibration and determination of these constants must be repeated at each temperature change. A DMA 48 by Anton Paar is used by the in-house analytical laboratory to perform these measurements. Density is then reported at four temperatures—5, 15, 30 and 60°C. A linear fit of the density versus temperature is developed, so that densities at arbitrary temperatures (within the range of 5-60°C) can be determined. A typical set of data is shown as Fig. 10.

MATHEMATICAL MODEL

The ASTM D4052 method gives the overall uncertainty of density in terms of repeatability, reproducibility and bias [19]. The uncertainties of the oscillation periods and/or constants themselves are not given. As a result, the mathematical model for calculating density (and constants) is not given here. Instead, the reader is reminded that the three specific uncertainties are additive in quadrature to get the combined density uncertainty and referred to ASTM's document on uncertainty [5]. The uncertainty in temperature during density measurements is mandated by the D4052 method. As with other curve fits, the weighted least squares method [13] is used to get an uncertainty in the fit parameters based on the uncertainty of the density and temperature. The calculated density is given by

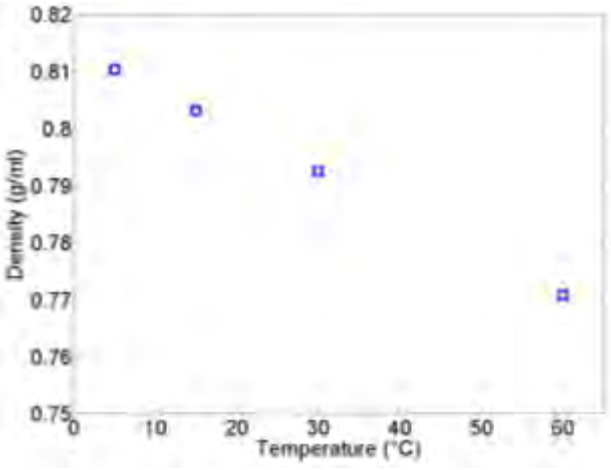

Figure 10. Density values as a function of temperature for a batch of fuel used in EC-1.

$$\rho = C_0 + C_1 T \tag{12}$$

The combined uncertainty, then, for the calculated density (at an arbitrary temperature with the 5 to 60°C range) is

$$u(\rho) = \sqrt{u^2(C_0) + T^2 u^2(C_1) + C_1^2 u^2(T) + 2T cov(C_0, C_1)} \tag{13}$$

Note that the temperature uncertainty used in the calculation of C_0 and C_1 is that associated with the DMA 48 used for the density measurement. The temperature used in (13), however, is the temperature measured during the EC-1 engine test.

SOURCES OF UNCERTAINTY

The DMA 48 maintains the temperature within the specified 0.05°C bounds through the use of a circulating water bath and a controller. Measurements are not made until the temperature of the sample has equilibrated to that of the bath. The ASTM method reports a repeatability of measurements and a reproducibility with 95% confidence intervals. They do not give the degrees of freedom for determining the interval, so a suitably large number of samples is assumed so that the specific uncertainty is 1/2 the given values (a sample greater than 61 points) [3]. The maximum bias listed in the ASTM method is used and listed in Table 7 below. The density of RP, the typical fuel used in EC-1, is comfortably within the range of densities for which the ASTM standard and given uncertainties apply.

COMBINED UNCERTAINTY

While the density is not used directly in the calculation of characteristic exhaust velocity or its efficiency, it is used in the mass flow rate as discussed below. The combined uncertainty for the density is dependent on the type and manufacturer of the thermocouple used in the system. Values range from 5.02×10^{-4} to 8.38×10^{-3} g/ml over the typical fuel temperature range (40-100°F) using Type E thermocouples. The Nanmac thermocouples result in combined uncertainties of 0.06% of the density while Omega thermocouples produce a range of uncertainties above this value but less than 0.11%.

As shown in Fig. 11, at low temperatures (or at all temperatures using the Omega thermocouples) the uncertainty is dominated by the uncertainty in fuel temperature during an engine firing. The methods to minimize the temperature uncertainty were addressed in a previous section. However, at higher temperatures, the uncertainty related to the curve fit dominates. (At 70°F the two are approximately equal contributors.) To lower the uncertainties associated with the curve fit, the uncertainty in density or temperature during the density measurement would need to be lowered or something would need to be done to increase the linearity of the measurements. Both of the uncertainties are quite low with the density measurement technique being the best found in the standards literature. Gains in this area are unlikely. However, without any improvements, the density values are quite well known with uncertainties on the order of the most accurate parameters examined.

Parameter	**Source of Uncertainty**	**Uncertainty Value**	**Distribution of Uncertainty**	**Degrees of Freedom**
Density (Measured)	Repeatability	$5x10^{-5}$ g/ml	Normal	>60?
Density (Measured)	Reproducibility	$2.5x10^{-4}$ g/ml	Normal	>60?
Density (Measured)	Total	$2.55\ x10^{-4}$ g/ml	Normal	>60?
Temperature (Density Measurement)	Total	0.05°C	Normal	>60?
Temperature (During Test)	Total	Nanmac 1.00-1.02% (T_{jun}-T_{record}) Omega 1.002°C		
C_0	Total	$2.1368x10^{-4}$	Normal	3
C_1	Total	$6.1995x10^{-6}$	Normal	3
Cov(C_0,C_1)	Total	$-1.0569x10^{-9}$	Normal	3
Density (Calculated)	Total	$5.02\text{-}4.72x10^{-4}$ g/ml (0.06%) $7.60\text{-}8.38x10^{-4}$ g/ml (0.09-0.11%)		

Table 7. Specific uncertainties for the density. Linear fit values are for Sample ID: RP2 20081229. C_0=0.8142, C_1=-7.2058x10^{-4}. The uncertainty in temperature during the test is for Type E thermocouples because that type is used for fuel measurements; totals are given for Nanmac (above) and Omega (below) thermocouples.

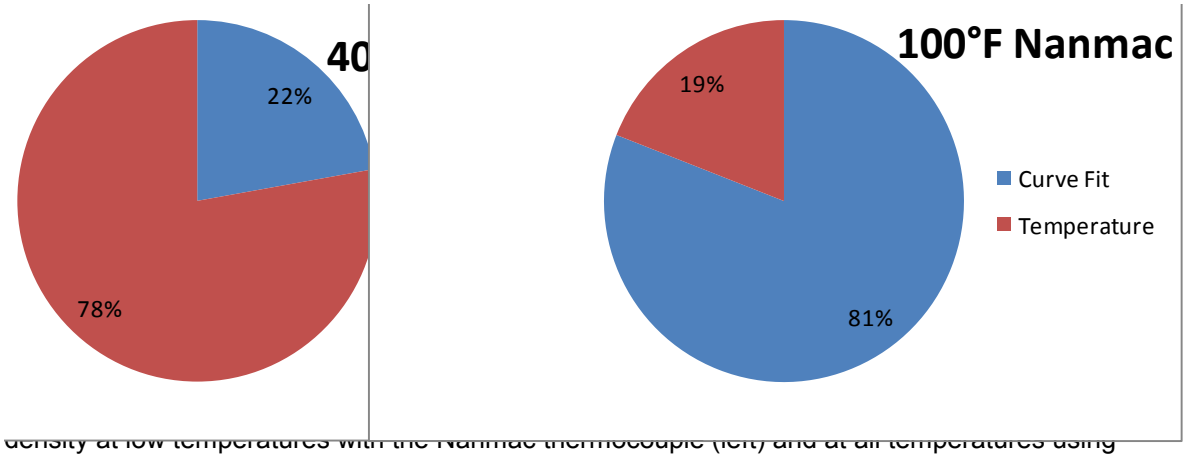

density at low temperatures with the Nanmac thermocouple (left) and at all temperatures using Omega thermocouples (not shown). At higher temperatures, the curve fit parameters become dominant; the uncertainty of these curve-fit parameters is related to the uncertainty in the ATMS D4052 procedure.

BEST PRACTICES AND ADDITIONAL CONCERNS

If the ASTM method is followed, there should be no uncertainty associated with a failure to measure the specific property of interest. The most likely source of an uncertainty of this type would be failure to properly clean and calibrate the instrument. ASTM D4052 has specific guidance for ensuring these errors do not occur. The important aspects of density measurement are

- Use well-characterized procedures, such as those laid out in ASTM D4052
- Select an instrument that meets the requirements within the above procedure
- Account for variations in density due to temperature. Failure to account for the variations in temperature produces errors; a 10°F difference in temperature can result in an error of approximately 1% in density.
- Choose a thermocouple type with low uncertainty; EC-1 uses a Type E.
- The weighted least squares method cited above is again recommended over a more traditional least squares method in order to produce uncertainty data from the curve-fitting procedure and include the uncertainties in both temperature and density in the curve fit.

VAPOR PRESSURE

BASIC PROCEDURE OVERVIEW

The vapor pressure measurements are made using a Grabner Minivap VP. This instrument uses a single expansion method as detailed in ASTM D6377 [20]. Essentially, this process uses a set pressure and volume of liquid, introduced to a chamber with a piston. The piston is then withdrawn to create an exact (larger) volume. The resultant pressure, following this volume increase, is reported. Temperature is controlled throughout by a thermoelectric module and high-precision RTD. Note, however, that details beyond the methodology, such as the stated uncertainties, are not applicable to EC-1 testing because typical rocket propellants have vapor pressures well below the stated range of applicability of D6377.

The in-house analytical laboratory reports vapor pressure at 5°C increments from 30 to 100°C. From these points a quadratic fit is calculated using a weighted least squares method, so that vapor pressure can be calculated at an arbitrary temperature within the measured range.

MATHEMATICAL MODEL

A quadratic fit is used to calculate the vapor pressure at an arbitrary temperature from 30 to 100°C

$$P_v = C_0 + C_1 T + C_2 T^2 \tag{14}$$

From this, the uncertainty in calculated vapor pressure is

$$u(P_v) = \sqrt{\begin{matrix}(C_1^2 + 4C_2^2T^2)u^2(T) + u^2(C_0) + T^2u^2(C_1) + T^4u^2(C_2) + 2Tcov(C_0, C_1) \\ +2T^2cov(C_0, C_2) + 2T^3cov(C_1, C_2)\end{matrix}} \tag{15}$$

SOURCES OF UNCERTAINTY

The manufacturer gives repeatability and reproducibility results for newer models of the process-instrument combination; however, these values are given at a single temperature (the standardized temperature of 37.8°C) and a pressure of 70kPa. A round-robin testing campaign gives the uncertainty as higher—these values are found in the ASTM D6377. However, this test campaign was at the single, standard temperature and for samples whose vapor pressures greatly exceeded those of typical rocket propellants—25kPa and up versus about 2kPa for RP. While it may be reasonable to assume that the effect of temperature on the uncertainty is low, the lower vapor pressure of RP versus the round-robin

Parameter	Source of Uncertainty	Uncertainty Value	Distribution of Uncertainty	Degrees of Freedom
Vapor Pressure (Measured)	Repeatability	1.24kPa	Normal	>60?
Vapor Pressure (Measured)	Reproducibility	2.13kPa	Normal	>60?
Vapor Pressure (Measured)	Total	1.705kPa	Normal	>60?
Temperature (Vapor Pressure Measurement)	Total	0.1°C	Normal	>60?
C_0	Total	6.1115	Normal	13
C_1	Total	0.2017	Normal	13
C_2	Total	1.5349×10^{-3}	Normal	13
Cov(C_0, C_1)	Total	-1.2075	Normal	13
Cov(C_0, C_2)	Total	8.8546×10^{-3}	Normal	13
Cov(C_1, C_2)	Total	-3.0628×10^{-4}	Normal	13
Temperature (During Test)	Total	Nanmac 1.00-1.02% (T_{jun}-T_{record}) Omega 1.002°C		
Vapor Pressure (Calculated)	Total	7.02-15.80 kPa		

Table 8. Specific uncertainties for the vapor pressure. Curve fit values are for Sample ID: RP2 20081229. C_0=2.7347, C_1=-0.0539, C_2=8.6296×10^{-4}. The uncertainty in temperature during the test is for Type E thermocouples because that type is used for fuel measurements; totals are applicable

samples is likely to introduce additional uncertainty. For example, from the analysis of pressures, above, it was concluded that the range of the pressure transducer should be close to the expected pressure range to minimize uncertainty. Since the instrument is designed expecting vapor pressures from 25 to 180kPa, but the sample has a vapor pressure closer to 2kPa, the pressure transducer is not be optimally ranged. On the other hand, chemicals with high vapor pressures are more volatile, and uncertainty can be introduced through handling of the sample and exposure to the atmosphere; the loss of volatile compounds is not an issue with kerosene propellants such as RP. Overall, then, in the absence of additional data, the uncertainties from D6377 will be used here. It should be noted, however, that these values are more speculative than conservative. A future program is investigating the repeatability of the in-house laboratory using RP fuels.

The manufacturer does not give uncertainties on the temperature. The temperature stability is given, but no uncertainty values. The D6377 method places limits on the accuracy and resolution, though. The total uncertainty in temperature will be considered to be the combined uncertainties in accuracy, resolution and stability.

COMBINED UNCERTAINTY

As with the density, the vapor pressure is not used directly in the calculation of c^* or efficiency, but it is used in the calculation of the liquid flow rate. The difficulty in measuring vapor pressure coupled with its low value makes this measurand extremely uncertain. However, improved methods were not discovered in the literature. The combined uncertainty in calculated vapor pressure is between 7.02 and 15.80 kPa over a temperature range of 40 to 100°F. This value is for a Type E thermocouple and is the same for either thermocouple manufacturer.

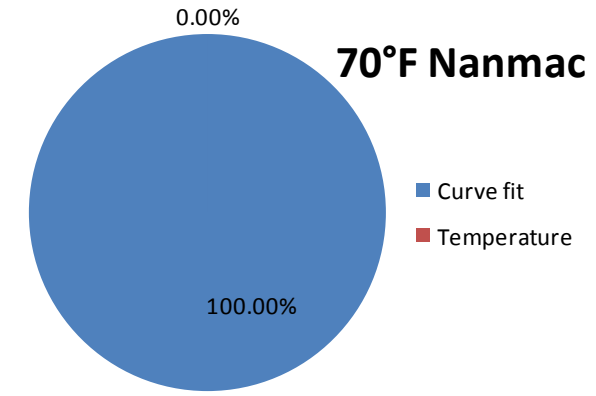

uncertainty at all temperatures. This representative graph is for the Type E Nanmac

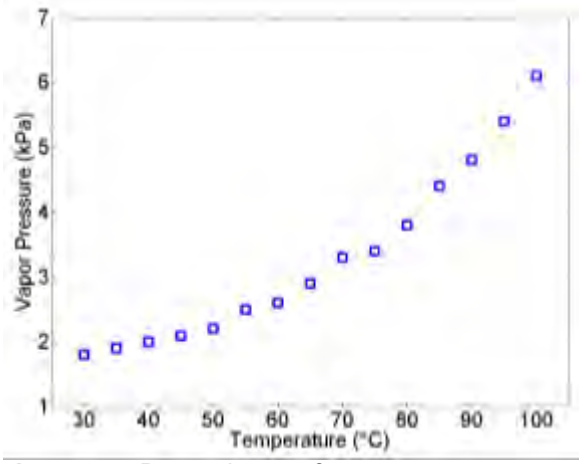

Figure 13. Dependence of vapor pressure on temperature for a fuel used in EC-1

Fig. 12 shows that the uncertainty is dominated by the contributions of curve fitting parameters. These uncertainties are, in turn, dominated by the uncertainty in vapor pressure. An in-house statistical analysis is underway which hopes to better calculate the uncertainty in the measurements of low vapor pressure fuels. It is hoped, but not yet known, that this investigation will lower the uncertainty in vapor pressure measurements. The contribution of the thermocouple temperature measurement uncertainty to the combined value is, at present, negligible.

BEST PRACTICES AND ADDITIONAL CONCERNS

The sampling of every batch of fuel and calculation of properties such as density and vapor pressure is important to ensure low overall uncertainty. The ASTM D6377 method should be used for vapor pressure measurements when possible instead of the D323 method due to the superior uncertainty levels of the former. The search for improved methods for nonvolatile fuels will continue. As with density, determining the vapor pressure at several different temperatures across the expected range is important. Failure to account for temperature changes of 10°C can result in bias of 10%. A typical plot of RP vapor pressure versus temperature, Fig. 13, illustrates the strong dependence on temperature.

LIQUID MASS FLOW RATE

BASIC PROCEDURE OVERVIEW

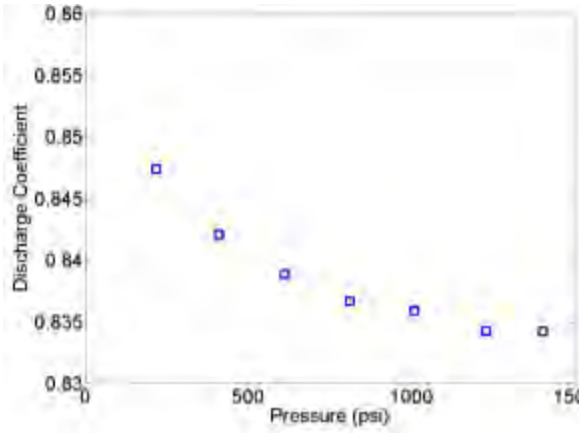

Figure 14. Discharge coefficient as a function of pressure for the 0.041 inch throat. (Values from water calibrations.)

EC-1 uses critical flow orifices to meter both the gas and liquid flows. For the liquid, the critical flow orifice is often called a cavitating venturi; that terminology will be used here. The determination of the flow rate is a multistep process. First, the venturi is calibrated to determine the discharge coefficient. The results from the calibration are fit to get a linear relationship between discharge coefficient and pressure. The calibration curve of the discharge coefficient is then used in the venturi equation to determine the flow rate at a given operating condition.

The discharge coefficient is determined using a catch-and-weigh setup. A computer interface is used to open a solenoid valve and start

a timer simultaneously. After a preset time elapses, which varies for different flow rates, the computer closes the valve and stops the timer. The captured liquid is weighed and divided by the elapsed time to generate a mass flow rate. The upstream pressure during the test is recorded. A discharge coefficient is calculated for a variety of upstream pressures (i.e., flow rates) by assuming a venturi throat and upstream pipe diameter. The small size of the venturi throats used in EC-1 (~0.03 to 0.07 inches) necessitates accounting for diameter changes via calibrating the discharge coefficient as opposed to measurement. The pin gauges, discussed above, would lead to a 1% or greater uncertainty in venturi throat diameter. Additionally, the discharge coefficient calibration procedure avoids any uncertainty associated with a change in circularity at the throat. Note that a slight additional uncertainty may result if the piping upstream of the venturi is replaced after calibration; however, the uncertainty in tubing diameter is substantially smaller than other uncertainties. The discharge coefficients for some of the cavitating venturis used in EC-1 have a weak dependence on pressure. As a result, a linear fit (using the weighted least squares method [13]) is used to quantify this relationship from the catch-and-weigh calibration. A sample result of discharge coefficient versus pressure is shown in Fig. 14. For each calibration, ten points are selected covering a range of pressures from 200 psi to either 2000 or 3000 psi. Water calibrations are performed up to 2000 psi, but fuel calibrations cover a range up to 3000 psi. The discharge coefficient determination process is repeated yearly. To date, changes in venturi throat diameter are not measurable via the pin gauges (i.e., <0.0005 inches). Changes in discharge coefficient over 5 years have been 1 to 2%.

In addition to upstream pressure, discharge coefficient and diameters, the density and vapor pressure of the liquid are needed to calculate mass flow rate. Each fuel is sampled and sent to our in-house analytical chemistry laboratory for analysis prior to testing. The procedures and uncertainties associated with determining these values are discussed above. When calibrations are performed using water, the water properties are taken from NIST webbook values [21].

Generally, the calibrations are performed using both water and the liquid fuel, typically RP-2 or RP-1. When fuels other than RP are used, calibrations with the actual fuel are not always feasible because of limited available quantities or low vapor pressures. Theoretically, the change in fuel can be accounted for with changes in vapor pressure and density. However, a factor the changes in the system and property differences is introduced, and differences have been observed experimentally. The differences likely stem from uncertainty in the fuel's density and vapor pressure as well as possibly being reflective of some real fluid effects such as boundary layer formation which are not well understood. Similar effects may be the cause of the pressure dependence of the discharge coefficient. Due to the two modes of operation, there are two similar uncertainty analyses, one considering each approach. In the first, the discharge coefficient is calibrated using water; in the second, the discharge coefficient is calibrated using RP-1. Following periods of heavy use, between scheduled yearly calibrations, the venturis are "spot checked" using water to verify discharge coefficients remain within tolerances.

MATHEMATICAL MODEL

The mass flow rate is calculated as a the mass caught over a given flow interval,

$$\dot{m}_{cw} = m/t \tag{16}$$

A standard cavitating venturi equation is used to calculate the discharge coefficient from the measured flow rate and upstream pressure with an assumed venturi and tubing diameter.

$$C_D = \frac{4}{\pi}\frac{m}{t}\sqrt{\frac{\left(\frac{1}{D_{ven}}\right)^4 - \left(\frac{1}{D_p}\right)^4}{2\rho(P - P_v)}} \tag{17}$$

where ρ and P_v are functions of temperature as detailed above.

A linear fit of the resultant discharge coefficient as a function of upstream pressure is developed using the weighted least squares method cited throughout this paper. The combined uncertainty in the discharge coefficient, including those in the mass flow rate measured from catch and weigh, and the

combined uncertainty in pressure (given above) are used in the weighted least squares method to get the uncertainty in the fit parameters.

$$u(C_D) = C_D \sqrt{\frac{u^2(m)}{m^2} + \frac{u^2(t)}{t^2} + \frac{u^2(\rho)}{4\rho^2} + \frac{u^2(P) + u^2(P_v)}{4(P - P_v)^2} + \frac{4}{\frac{1}{D_{ven}^4} - \frac{1}{D_p^4}}\left[\frac{u^2(D_{ven})}{D_{ven}^{10}} + \frac{u^2(D_p)}{D_p^{10}}\right]} \tag{18}$$

This curve fit is, in turn, used with the values of upstream pressure measured during a test to calculate the mass flow rate. There is no uncertainty in the venturi diameter because that value is assumed to be known exactly and any deviations are accounted for in the calibrated discharge coefficient value. Similarly, if the calibration is performed in the system of use, the uncertainty in the piping diameter is zero because it is accounted for in the discharge coefficient; both are included here for completeness, but their values are set to zero in the calculations. Values for the specific uncertainties in (18) are given in Table 9.

The equation for mass flow rate is then

$$\dot{m}_{fuel} = \frac{\pi}{4}(C_0 + C_1 P)\sqrt{\frac{2\rho(P - P_v)}{\left(\frac{1}{D_{ven}}\right)^4 - \left(\frac{1}{D_p}\right)^4}} \tag{19}$$

Considering (19), the combined uncertainty for the mass flow rate is

$$u(\dot{m}_{fuel}) = \dot{m}_{fuel}\sqrt{\begin{aligned}&\frac{u^2(C_0) + P^2u^2(C_1)}{(C_0 + C_1P)^2} + \frac{u^2(\rho)}{4\rho^2} + \frac{u^2(P_v)}{4(P - P_v)^2} + \frac{4}{\frac{1}{D_{ven}^4} - \frac{1}{D_p^4}}\left[\frac{u^2(D_{ven})}{D_{ven}^{10}} + \frac{u^2(D_p)}{D_p^{10}}\right]\\ &+ \frac{[C_0 + C_1P + 2C_1(P - P_v)]^2}{4(P - P_v)^2}u^2(P) + \frac{2P}{(C_0 + C_1P)\dot{m}}cov(C_0, C_1)\end{aligned}} \tag{20}$$

Values for these specific uncertainties are given in Table 10 and shown in Figure 15. Note that the uncertainty in tubing size is only relevant in the situation where venturis are calibrated only in AFRL's water flow facility and not in the system using the fuel, and, due to the procedure followed here, the uncertainty in venturi diameter is again zero as there is no change in venturi from the calibration to the use.

The only uncertainties which should be covariant in these formulations are the fit parameters. The covariance is obtained from the fitting procedure.

SOURCES OF UNCERTAINTY

The catch-and-weigh procedure has uncertainty associated with the determination of the mass as well as the elapsed time measurement. The scale used to weigh the liquid is either an Ohaus I-10 with a B-100S base or an A & D HP-30K. The A & D HP-30K is used at AFRL's cold flow facility when calibrations are performed using water; the other is used for calibrations with the fuel. The run certainties for each scale are given in Table 9. The scales are calibrated to manufacturer's specifications by a commercial company yearly. (Calibrations are NIST traceable.) The timer is controlled via the controller software that opens the valve. The timer starts when the signal to open the valve is initiated. This situation results in some uncertainty due to finite opening time of the valve. Similarly, the timer stops when the signal to close the valve is initiated. The valves in use in both the cold flow and EC-1 facilities have typical open (or close) time under 20 ms. During opening and closing, some amount of mass flow, lower than the target flow rate, occurs. As a rough estimation, assume that the flow through the valve varies linearly with percentage open (this is a worse case, as the valves used in the system are fast response valves). A linear response would translate into half the total flow during the opening phase compared to once the valve is fully open. Assume the same situation occurs during closing. Theoretically, this deficit could be corrected for in the measured mass flow rate; however, the exact response is not known and may vary from test to test, so it is included instead as an uncertainty. The timing is automated to eliminate user-introduced uncertainty and reaction times. With the automated

Parameter	Source of Uncertainty	Uncertainty Value	Distribution of Uncertainty	Degrees of Freedom
Mass	Resolution (Ohaus/A&D)	0.005 lb / 0.05g	Uniform	Infinite
Mass	Manufacturer (Ohaus/A&D)	0.01 lb / .3 g		
Mass	Valve Delay	$\dot{m} * 0.04s$		
Mass	Total (in lb)	$0.01\sqrt{1.25 + 16\dot{m}^2}$ $0.01\sqrt{0.0045 + 16\dot{m}^2}$		
Time	Resolution	0.005 s	Uniform	Infinite
Time	Valve Actuation	0.04 s		
Time	Total	0.0403 s		
Diameter (Venturi)	Total	0 inch	N/A	N/A
Density (Fuel)	Total	5.02-4.72x10^{-4} g/ml 7.60-8.38x10^{-4} g/ml		
Density (Water)	Total	0 g/ml	N/A	N/A
Vapor Pressure (Fuel)	Total	7.02-15.80 kPa		
Vapor Pressure (Water)	Total	0 kPa	N/A	N/A
Pressure	Total	0.28 to 0.45 psi		
Discharge Coefficient (Water)	Total	0.06-0.14%		
Discharge Coefficient (Fuel)	Total	0.07-0.41% Nanmac 0.08-0.41% Omega		

Table 9. The specific uncertainties for the discharge coefficient for the cavitating venturis is given. Mass varies from 10 to 30 lb with flow times from 80 to 135 seconds keeping mass flow rates between 0.10 and 0.35 lb/s. Supply pressures from 300 to 2000 are considered as well as a temperature range of 40°-100°F for the propellants (for density and vapor pressure). Trends are discussed in the combined uncertainty subsection. The assumptions that the uncertainties in the water properties are negligible are preliminary, but aid in showing some trends.

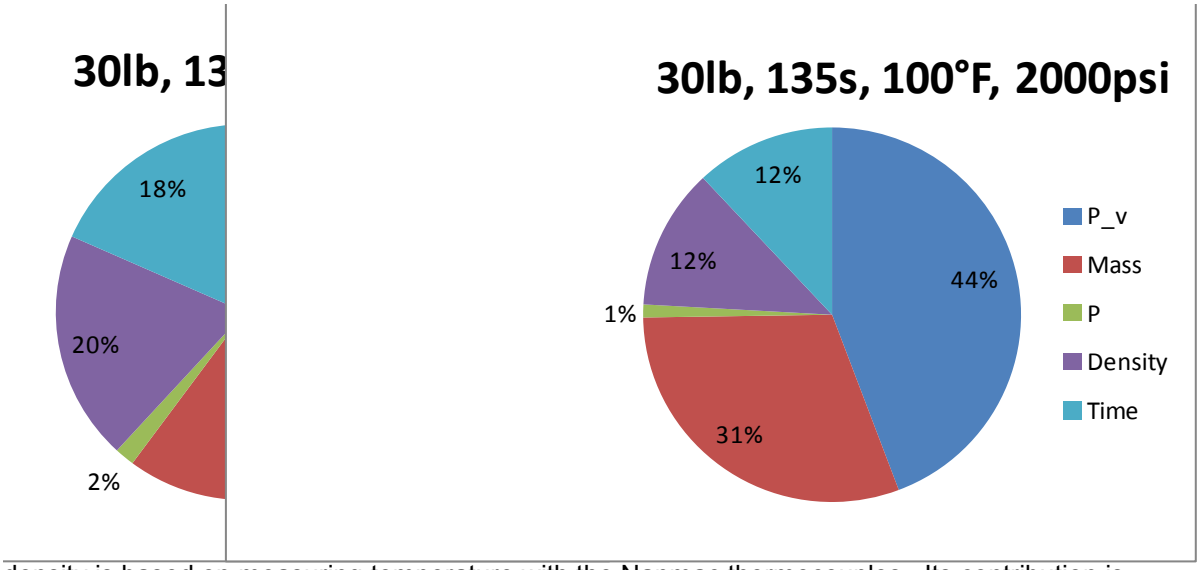

density is based on measuring temperature with the Nanmac thermocouples. Its contribution is approximately doubled when Omega thermocouples are used. When the pressure decreases to 300 psi, the vapor pressure dominates, being >85% of the uncertainty for most of the range of other variables.

Parameter	Source of Uncertainty	Uncertainty Value	Distribution of Uncertainty	Degrees of Freedom
Diameter (Venturi)	Total	0 inch	N/A	N/A
Diameter (Tubing)	Total	8.315×10^{-3} inch		
Density (Fuel)	Total	$5.02\text{-}4.72 \times 10^{-4}$ g/ml $7.60\text{-}8.38 \times 10^{-4}$ g/ml		
Vapor Pressure (Fuel)	Total	7.02-15.80 kPa		
Pressure	Total	0.28 to 0.45 psi		
C_0 (Water)	Total	2.8033×10^{-4}		
C_1 (Water)	Total	-2.1416×10^{-7}		
C_0 (Fuel)	Total	1.6255×10^{-3}		
C_1 (Fuel)	Total	7.1015×10^{-7}		
Cov(C_0, C_1) (Water)	Total	-5.556×10^{-11}		
Cov(C_0, C_1) (Fuel)	Total	-1.0975×10^{-9}		
Mass Flow Rate (using Water cal)	Total	0.68-0.78%		
Mass Flow Rate (using Fuel cal)	Total	0.35-0.51%		

Table 10. The contributions to the combined uncertainty in mass flow rate for the cavitating venturis. The curve fit parameters are for the 0.041 venturi used in EC-1 (chosen at random for analysis here). For the water calibrations the slope, C_1, is -4.5197×10^{-6} and the intercept is 0.8413. For the fuel calibrations C_1=-6.0087×10^{-8} and C_0=0.8309. The uncertainty in tubing diameter is for ½" (OD) 0.083 wall thickness tubing per T.O. 00-25-223.

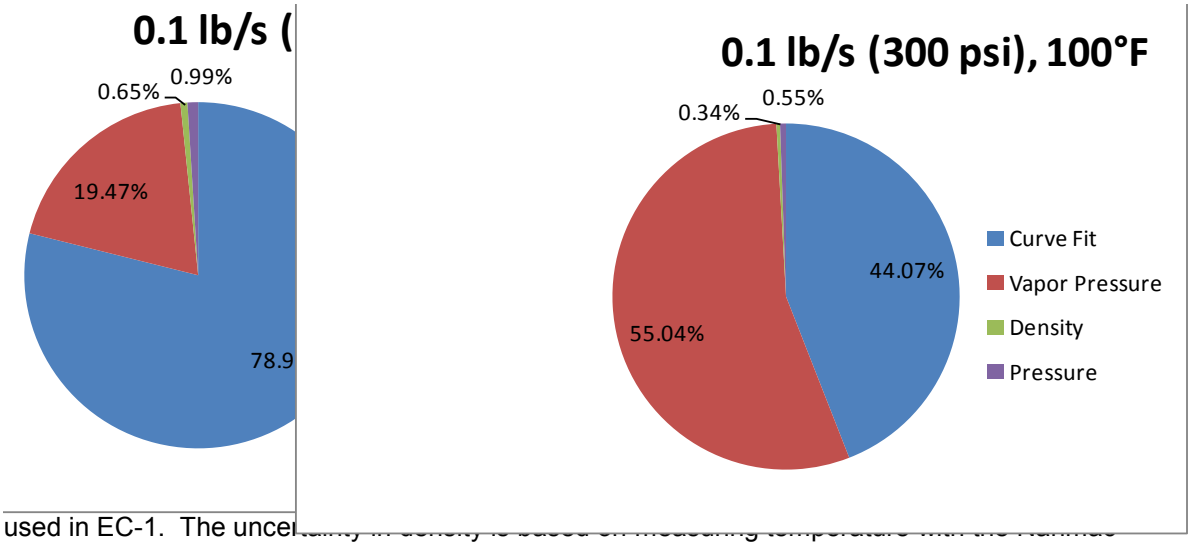

used in EC-1. The uncer[illegible] thermocouples. There is little change for the Omega thermocouple. At higher driving pressures, the uncertainty in the curve fit is overwhelmingly dominant—over 99% at 2000 psi.

system, the only considered uncertainties are those associated with resolution and valve initiation, since others, such as computer time keeping, are orders of magnitude less than the resolution. The valve initiation time coupled with the loop time of the DAQ system is typically 20 ms or less for the valves in use; therefore, the flow time and recorded time could be off by as much as 40 ms, 20 ms each for opening and closing. Obviously, the percentage uncertainty in both mass and time can be minimized by increasing the flow time during calibration. The EC-1 facility is limited in time and volume of fuel available. The length of the calibration can be no longer than 327 seconds in order to maintain the millisecond resolution on the DAQ system. This period includes an initial 15 seconds to produce steady

flow before switching the flow to the weigh-bucket and the shut down time. The fuel tanks hold either 5 or 10 gallons of fuel at a maximum (depending on the tank), so calibration mass is limited by this volume. Generally, attempts are made to be near, with a comfortable margin, one of these two limits—typically just under 300 seconds of run time or 4 gallons of fuel, whichever results in the smaller mass/shorter run time.

Uncertainties associated with density and vapor pressure determinations have their own sections above. The combined uncertainty for each is given again, for easy reference, in the tables below. The uncertainty in the water density at isobaric conditions is considered negligible. The uncertainty in water vapor is not given; furthermore, the information given in the NIST webbook is a curve fit not the data itself [21]. In the current work, this is neglected; however, the likelihood that this value is truly negligible is small. Since most calibrations are performed with fuel, this assumption does not impact the recent work in and analysis of the EC-1 engine. Note that both the fuel and water properties are considered to be isobaric (at 1 atm) and neglect the effects of pressure on density. Again, this uncertainty is neglected in the current analysis. The uncertainty in measured pressure has also been detailed in a previous section with the combined uncertainty reproduced in the tables.

As stated above, it is not always possible to calibrate using the fuel. In these cases, the calibration is performed with water at an in-house cold-flow facility. Because this facility is separate from EC-1, the uncertainty in tubing diameter must be considered. While this diameter could be measured via pin gauges, EC-1 relies on the tolerances provided by the manufacturer as an estimate of the uncertainty. Batches of tubing have been spot-checked at various times and found to fall within the provided tolerance band given by the Air Force Technical Order (T.O.) covering pressure systems [22].

COMBINED UNCERTAINTY

Unlike previous measurands considered, the discharge coefficient and mass flow rates depend on a number of other measurands in complex ways. Many of these measurands vary from test to test, so giving a combined uncertainty is challenging. A range of parameter values was examined based on typical values for EC-1. The collected mass ranged from 10 to 30 lb with times from 80 to 135 seconds (these are typical for fuel calibrations). The pressure ranged from 300 to 2000 psi. The vapor pressure and density vary with temperature, so a range from 40° to 100°F was examined.

The range of uncertainties in discharge coefficient is given in Table 9. The two largest contributors are typically the vapor pressure and the mass. These alternate in dominance depending on the conditions. The combined uncertainty in discharge coefficient is a minimum at the highest mass and collection times with the largest pressure and lowest temperature. In general, it would be recommended to run at elevated pressures and low temperatures and to collect as much mass over as long a time as possible. In reality, the upstream pressure, mass and time are limited by the venturi diameter and amount of fuel available. Similarly, controlling fuel temperature is difficult or impossible in most systems. In EC-1 it is somewhat controllable only by selecting the time of year in which the calibrations are performed. A recommendation can be made to use a smaller venturi size to get a higher upstream pressure for a given flow rate, but higher driving pressures do increase wear on the venturi and the higher pressures may not always be achievable depending on how the propellant system is pressurized. The uncertainty in vapor pressure cannot be controlled, but if it could be reduced then the dependence on pressure and temperature would decrease dramatically. At low pressures the vapor pressure completely dominates the uncertainty. It should also be noted that the lowered uncertainty in pressure created by changing transducers and other updates, has decreased the combined uncertainty in discharge coefficient appreciably. Using the earlier values (from a randomly selected transducer) of ~9psi uncertainty more than triples the combined uncertainty—0.23-1.55%.

Two similar combined uncertainties are considered here. In an ideal case, the fuel is used to calibrate the discharge coefficient. Results are given here for a randomly selected venturi from those typically used in EC-1, one with a 0.041 inch diameter throat. Using (20), fuel calibration results in an uncertainty of 0.35 to 0.51% of the mass flow rate (higher uncertainties at higher flow rates and temperatures) for the fuel flow rates. For tests involving RP fuels, EC-1 operates in this mode of calibrating with the fuels being used for testing. In the case where only small quantities of fuel are available or they are too volatile to use for flow calibrations, water is used to calibrate the discharge coefficient while the fuel properties are used in the final mass flow rate equation (20). This procedure

results in a combined uncertainty of 0.68 to 0.78% of the mass flow rate. Note that in this case the uncertainty in pipe diameter, as given in Table 10, is used while it is zero in the earlier case where fuel calibrations are performed (the tubing there being unchanged). Obviously, calibration with the testing fuel reduces the uncertainty in mass flow rate. Furthermore, the uncertainty in tubing diameter is a nonnegligible contribution. This uncertainty can be reduced by making measurements of the piping. As a result of the analysis, this step has been added to the calibration procedure when calibrations are performed using water.

The two largest contributors are the curve fit parameters (in other words, the uncertainty in discharge coefficient) and the vapor pressure. In general, the combined uncertainty is lower at lower flow rates and temperatures. Furthermore, operating at lower flow rates means that the discharge coefficient has a large contribution to the uncertainty. Since this specific uncertainty may be reduced more easily than the vapor pressure uncertainty, it would be the area to target for any further improvement. A major improvement, however, has already been achieved through reduction in the uncertainty in pressure measurements. Using previous transducer numbers results in a doubling, or more, of the combined uncertainty versus the current number. The present numbers for mass flow rate are likely to be as low as practically achievable.

BEST PRACTICES AND ADDITIONAL CONCERNS

With the mass flow there is less ambiguity that what is being measuring is the parameter of interest than there is with measurements such as temperature and pressure. However, there are some additional complications that should be considered. Often, fuels and water have gases dissolved within them. Due to the large pressure drop associated with cavitating venturis, dissolved gases can come out of solution leading to bubbly flow. Investigations of the effect of dissolved gases on measured mass flow rates were made in AFRL's cold flow facility. Comparisons between the standard deionized water (containing dissolved air) with water degassed in a tank which was under vacuum for some time (no dissolved air) resulted in no measurable difference in mass flow rate. The downstream flow did change from bubbly to clear, however. While it can be important to ensure that downstream flow is not bubble-laden, the dissolved gases do not appear to have a measurable effect in the flow rate in this system. To help minimize bubble-laden flow, though, bladder tanks are used in EC-1 so that the pressurizing nitrogen head is not in direct contact with the fuel.

Well-behaved flow rates over a pressure range depend on sufficient upstream and downstream runs so that the flow entering the venturi is well-developed. ISO 5167 requires sufficient upstream distances to ensure the flow is swirl free and fully developed [23]. EC-1 has a straight run >20D upstream and >13D downstream of the venturis. Proper distances are especially important if the discharge coefficient is being calculated on a system which is not the test system because the upstream and downstream distances can impact the flow rates if they are insufficient [23].

From these considerations, experience and the uncertainty analysis the following practices are recommended

- The discharge coefficient changes over time due to surface roughening and possible erosion of the venturi, so periodic recalibration is needed
- Periodic calibration of the discharge coefficient with an assumed constant diameter is recommended; do not rely on measurements of the throat diameter and assume discharge coefficients are unchanged
- Due to the small diameters of the venturis, small uncertainties in the diameter translate into large uncertainties in mass flow rate (see the sensitivity factor in (20))
- To establish a period of calibration, periodic spot checks of the discharge coefficient can be carried out either with fuel or with water
- The largest practical mass and time frame should be collected during calibrations to minimize the uncertainty impact on discharge coefficient
- If possible, calibrations should be conducted in the experimental system with the fuel
- Any efforts taken to reduce the uncertainty in temperature (related to the density and vapor pressure determination) and pressure will pay off in reduction in mass flow rate uncertainty

- A minimum upstream straight length of at least 10D and a minimum downstream straight length of ~5D should be provided around the venturi
    - If these lengths cannot be accommodated, it is imperative that discharge coefficient being calibrated in the system with the fuel (or an identical flow path be constructed for calibrations)
- Weighted least square methods should be used for curve fit in order to provide uncertainties and covariances; the chosen method should include uncertainty in both of the fitted parameters
- While shown to not impact the measured values, it is often appropriate to reduce the likelihood that fuel has or will absorb gases, especially if the propellant is driven by tank pressurization. The use bladders in run tanks is therefore recommended.

GAS MASS FLOW RATE

BASIC PROCEDURE OVERVIEW

In EC-1 the gas flow is metered using a critical flow nozzle, referred to hereafter as a sonic nozzle. The sonic nozzles have been calibrated, in-house, in the past using a catch-and-weigh technique similar to that described above for the cavitating venturis. As with the venturis, a calibration of the discharge coefficient is performed and those results are used in the sonic nozzle mass flow equation. In the case of the gas, however, the buoyant force is considered for determination of the captured (flowed) mass and the uncertainty associated with this measurement is, therefore, somewhat higher than when weighing liquid. More recently, a select group of sonic nozzles were sent to an outside agency (CEESI) for calibration. The results of their calibration agreed, well within estimated uncertainty bands, with the in-house measurements. Currently, the venturis not sent to CEESI have been calibrated in-house using an "in-line" system. A CEESI-calibrated nozzle is placed upstream of the nozzle being calibrated, ensuring sufficient distance between the two sonic nozzles for flow recovery and redevelopment. A known mass flow rate is set by the upstream nozzle, the system is run until a steady temperature is achieved prior to the second nozzle, and the pressure at the second nozzle is recorded. The known flow rate, pressure and temperature are then used to calculate a discharge coefficient. In the sonic nozzles, unlike the cavitating venturis, no dependence of discharge coefficient on pressure has been observed, so a straight average of the points is used and a Type A analysis is currently used to determine the uncertainty. Five to six flow rates over the overlapping range of the two nozzles are recorded. As with the cavitating venturis, the physical dimensions of the sonic nozzle are assumed to be constant. Calibrations are performed using nitrogen. The recalibration cycle is three years to CEESI and yearly in-house. The sonic nozzles calibrated at CEESI are not or are rarely used for testing. The uncertainties in discharge coefficient associated with the in-line calibration will be considered here: the catch-and-weigh procedure is no longer being used due to its complexity and availability of appropriate equipment. However, the data given here and in the prior section should be sufficient to make an estimate of the uncertainties associated with that procedure as applied to sonic nozzles. The uncertainty in mass associated with buoyancy in the catch and weigh procedure was approximately 5 grams.

Once the discharge coefficient (and assumed nozzle throat area) are known, the mass flow rate can be calculated for oxygen using the upstream pressure and temperature and the critical flow factor for oxygen. During the calibration, with nitrogen, the critical flow factor is calculated using the curve fit provided by Stewart et al. [24]. They do not provide a value for oxygen, however. Oxygen's properties from REFPROP [21] were used along with Stewart's procedures to generate a curve fit of the critical flow parameter as a function of pressure and temperature. The equation and constant values for the calculation of oxygen's critical flow parameter

$$C_{FF} = \sum_{n=0}^{5} a_n P^n \text{ with } a_n = \sum_{j=0}^{5} b_{n,j} T^j \tag{20}$$

MATHEMATICAL MODEL

The equation for flow rate through a sonic nozzle is

$$\dot{m}_{ox} = \frac{A_{sn} C_D C_{FF} P}{\sqrt{RT}} \tag{22}$$

The typical nomenclature for the critical flow factor is C^*; however, to avoid confusion with the characteristic velocity, c^* the critical flow factor will be designated C_{FF}. The above equation is solved for discharge coefficient during the calibration. The uncertainty in discharge coefficient can be calculated from (22)

$$u(C_D) = C_D \sqrt{\frac{u^2(A_{sn})}{A_{sn}^2} + \frac{u^2\left(\dot{m}_{ox,supply}\right)}{\dot{m}_{ox,supply}^2} + \frac{u^2(C_{FF})}{C_{FF}^2} + \frac{u^2(P)}{P^2} + \frac{u^2(R)}{4R^2} + \frac{u^2(T)}{4T^2}} \tag{23}$$

As with the throat diameter in the cavitating venturis, the area of the sonic nozzle throat is assumed to be known and the uncertainty associated with it is zero. The uncertainty in the gas constant is also assumed to be negligible here as it is well established in the literature (uncertainty of 7.5x10-6 J/mol.K; R=8.3144621 J/mol.K per 2010 CODATA recommended values [25]).

The combined uncertainty in mass flow rate is

$$u(\dot{m}_{ox}) = \dot{m}_{ox} \sqrt{\frac{u^2(A_{sn})}{A_{sn}^2} + \frac{u^2(C_D)}{C_D^2} + \frac{u^2(C_{FF})}{C_{FF}^2} + \frac{u^2(P)}{P^2} + \frac{u^2(R)}{4R^2} + \frac{u^2(T)}{4T^2}} \tag{24}$$

Again, the gas constant and its uncertainty are included for completeness along with the throat area. The throat area will be neglected as it is an assumed value in the calibration of discharge coefficient and remains unchanged from calibration to test.

There could be some covariance between the critical flow factor and the pressure and temperature, since that factor is a function of those parameters. However, the reference from which the C_{FF} is derived does not address this issue, and the determination of the covariance is not clear. As a result, these covariances will be neglected. Note that this omission may lower the calculated combined uncertainty, but the effect is expected to be small and, as such, tolerable in the absence of any additional information to estimate the parameter. No other covariances exist.

SOURCES OF UNCERTAINTY

As with the venturis, the throat area is assumed to be a given value during the discharge coefficient calibration. The sensitivity of the gas flow rate to the uncertainty in area is less than for the liquid flow rate, but the calibration of the discharge coefficient to account for any changes still has a lower uncertainty than measuring the throat area and assuming a discharge coefficient. It also prevents additional, difficult to define, uncertainty due to noncircularity. Still, there are additional effects other than those considered here that impact the repeatability of the discharge coefficient measurement. As a result, the multiple points are used for a Type A analysis to get repeatability.

There is an uncertainty in the mass flow rate set point used for calibration. This depends on the technique being used during calibration. The value cited in Table 11 is that associated with the calibration performed by CEESI. If a catch-and-weigh technique was used, an analysis similar to the liquid mass flow catch-and-weigh analysis could be used. Note, however, that in this case an additional term due to buoyancy would likely need to be added.

The uncertainty in the critical flow factor for nitrogen is the number given in the paper by Stewart et al. [24] and mostly reflects uncertainties introduced by fitting a curve to the tabular values. There is an additional uncertainty here introduced by large values of the nozzle throat-to-pipe diameter ratio. The values given in Stewart's work apply for ratios up to 0.15; however, in EC-1 the ratios can be as high as 0.2 (typically 0.07 to 0.2). In a follow-on work, Stewart et al. reported on the effect of the diameter ratio on the mass flow rate [26]. The correction given accounts for the use of static pressure measurements

and typical in-flow temperature measurements (somewhere between static and stagnation, typically). The static pressure and directly measured temperature are used in the EC-1 calculations. Based on Stewart's work, failure to correct to the stagnation pressure and temperature could introduce significant uncertainty at high diameter ratios. However, EC-1 has only moderate diameter ratios and, as seen in the Figs 17 and 18, the uncertainty related to the critical flow factor is negligible. EC-1 does not correct for the velocity at the measurement location when calculating flow rate. To account for the error this produces, a factor $u^2(S)/\dot{m}^2$, equal to the correction factors cited above, should be added under the radical in (24) Note that the incompressible nature of the liquid along with substantially decreased diameter ratios of throat-to-pipe diameter render this error negligibly small in the case of the cavitating venturis.

Stewart's work does not give values for critical flow factors of oxygen [24], so a procedure similar to the one laid out in that work was used to calculate the values for oxygen. These values were then curve fit using a least squares approach and a form given in (21). The property values for oxygen are well established. As with the critical flow factor for nitrogen, the uncertainty is related to the curve fit of the results. That is difficult to assess and has currently not been accomplished. A program is being written to directly calculate critical flow factors from REFPROP (or NIST webbook) data. This program will also take into account the changes for high pipe-to-throat diameter ratios. The remaining uncertainty will be that associated with not knowing the recovery factor for the thermocouple and the uncertainties in property values. The latter of which should be negligible. Because no assessment of the current uncertainty has been done, values will be assumed to be close to (rounded up from) those for the nitrogen curve fits. Given that, as shown in the figures and tables below, the values would have to be substantially larger than the nitrogen values to have any effect on the combined uncertainty, this assumption appears justified.

The uncertainty in pressure and temperature is addressed in detail above and the combined uncertainties in each are included in Table 11 for easy reference.

Parameter	**Source of Uncertainty**	**Uncertainty Value**	**Distribution of Uncertainty**	**Degrees of Freedom**
Throat Area	Total	0 inch^2	N/A	N/A
Mass Flow Rate (Supplied)	Total	0.15% of m (maximum)		
Critical Flow Factor (N2)	Total	0.005% of C_{FF} (maximum)		
Critical Flow Factor (O2)	Total	0.005% of C_{FF}		
Correction Factor (N2)	Total	0.043% of m (maximum)		
Correction Factor (O2)	Total	0.05% of m		
Pressure	Total	0.28 to 0.45 psi		
Temperature	Total	Nanmac 1.00-1.02% (T_{jun}-T_{record}) Omega 1.002°C		
Discharge Coefficient	Total (includes Repeatability)	6.91-0.41% Nanmac 11.3-1.34% Omega		
Mass Flow Rate	Total	9.77-0.56% Nanmac 15.9-1.88% Omega		

Table 11. The specific uncertainties which apply to the discharge coefficient and mass flow rate uncertainties using the sonic nozzles. A range of conditions are considered for pressure, mass flow rate during calibration, and temperature over the typical ranges. Mass flow rates from 0.15 to 0.80 lb/s are considered. Uncertainty falls as the temperature increases.

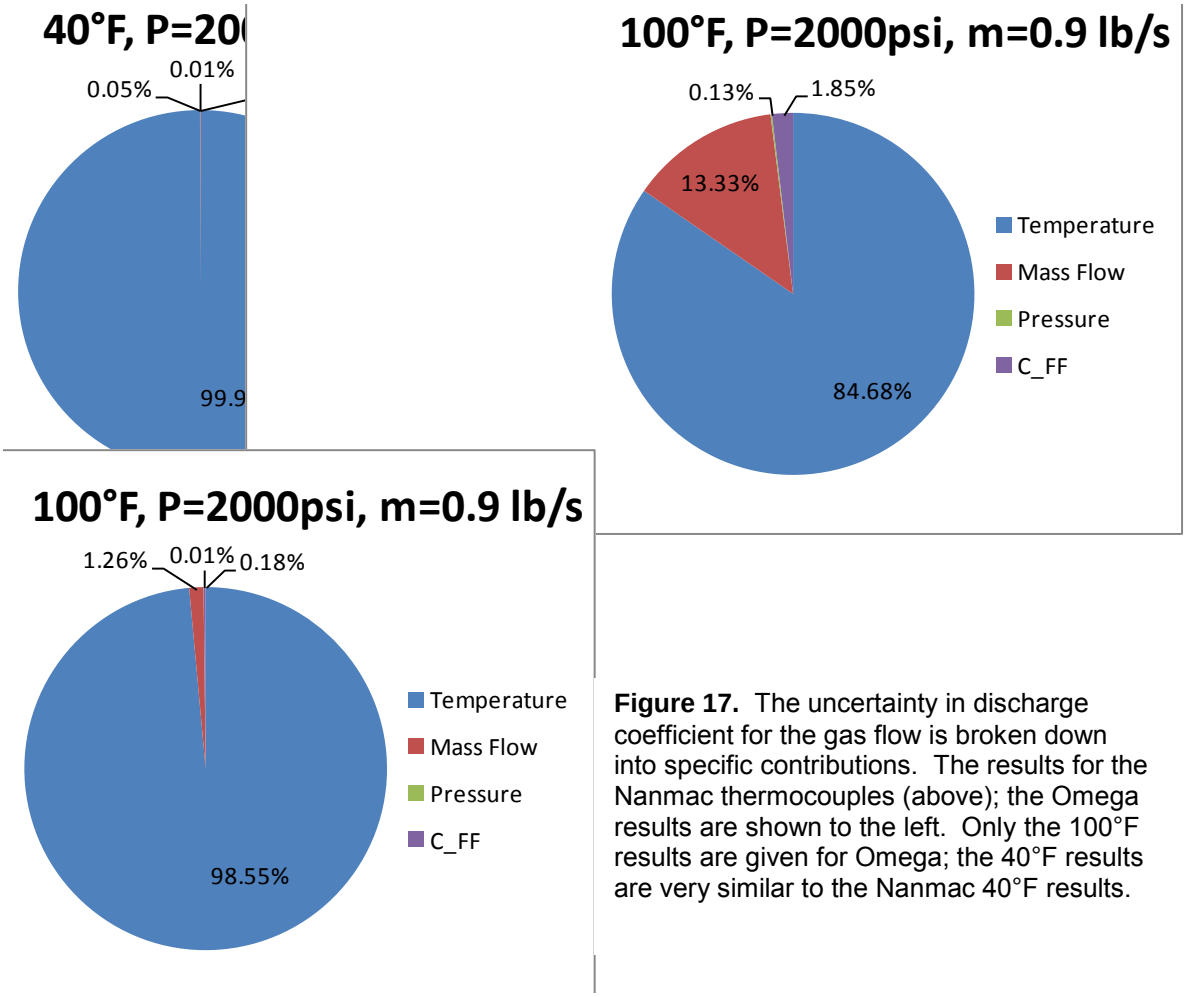

Figure 17. The uncertainty in discharge coefficient for the gas flow is broken down into specific contributions. The results for the Nanmac thermocouples (above); the Omega results are shown to the left. Only the 100°F results are given for Omega; the 40°F results are very similar to the Nanmac 40°F results.

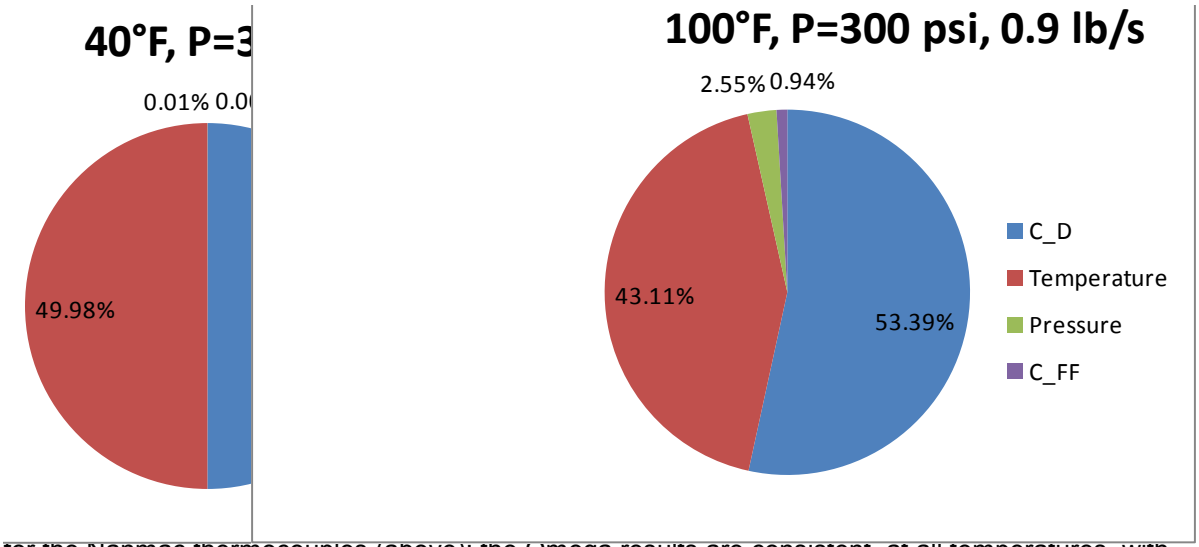

for the Nanmac thermocouples (above); the Omega results are consistent, at all temperatures, with the 40°F Nanmac results.

COMBINED UNCERTAINTY

The combined uncertainty in mass flow rate is 0.56 and 15.9% of the mass flow rate dependent on temperature and the type of thermocouple used (see Table 11) The uncertainty increases as the temperature decreases. It is only very weakly dependent on other inputs. The analysis shows that the uncertainty in the critical flow factor and any adjustments due to large contraction ratios can be neglected. However, given the relative ease in calculation, EC-1 is moving away from using curve fits of this factor which will reduce its contribution even further. This finding also highlights that there is negligible additional uncertainty introduced by calibrating with nitrogen (since its properties are well known) versus calibrating with oxygen. The pressure contribution is also negligible here. However, with previous pressure transducers (whose uncertainty, given above was ~ 9 psi) the pressure contribution was significant contributing to between 8 and 50% of the combined uncertainty (higher contributions at higher pressures).

The remaining uncertainty is largely dominated by temperature and discharge coefficient (Fig.

The remaining uncertainty is largely dominated by temperature and discharge coefficient (Fig. 18), especially at the lower temperatures. Because the temperature decreases as gas expands, it is not unusual to calibrate in these low temperature ranges. Operating temperature ranges tend to be higher on average. The discharge coefficient is, again, dominated by temperature measurements (Fig. 17). It would, then, be recommended to calibrate and operate at higher temperatures to reduce uncertainty. This recommendation is not practically achievable in most engine systems, however. As a result, the only recommendations can be to reduce the temperature uncertainty as much as possible by following the guidelines above.

BEST PRACTICES AND ADDITIONAL CONCERNS

If the above procedure is followed, there should be little additional uncertainty that the flow rate measured is the flow rate through the engine. As with the cavitating venturis, it is important to provide sufficient upstream length to ensure the flow is smooth and developed heading into the sonic nozzle [23]. EC-1 has a >28D length upstream along with flow straighteners and a 13.5D length downstream. With the sonic nozzles care also must be taken to avoid compression at start up. If a valve is located upstream of the nozzle and it is quickly opened, the gas between the valve and sonic nozzle is compressed leading to a sharp spike in temperature and pressure. This spike makes the upstream temperature more uncertain than the simple instrumentation analysis given here. In fact, the short run times in EC-1 and the time constants of the thermocouples can produce a situation where the thermocouple does not relax from the initial spike and never measures the true gas temperature during the steady state period of the test. Obviously, this uncertainty in temperature creates an uncertainty in the mass flow rate. Positioning the valves downstream of the sonic nozzles mitigates this problem.

The following steps should be taken to achieve and maintain low uncertainties in gas flow rate measurement

- Calibrate periodically to account for wear that changes the discharge coefficient of the sonic nozzle
- Use a critical flow factor which takes into consideration real gas effects
- While EC-1 uses a specific procedure [24], there are several in the literature which produce very similar values and uncertainties
- Provide sufficient development length upstream of the nozzle
- Corrections for this could be included in the discharge coefficient, but then the coefficient would likely become a function of pressure
- If the throat-to-pipe diameter is large, typically above 0.15 [26], make corrections to the critical flow factor to account for the upstream velocity
- Locate valves downstream of the sonic nozzle to avoid sudden compression upstream of the nozzle.
- Any efforts taken to reduce the uncertainty in temperature and pressure will pay off in reduction in mass flow rate uncertainty

MIXTURE RATIO AND TOTAL MASS FLOW RATE

BASIC PROCEDURE OVERVIEW

The mixture ratio is determined from the measured oxidizer (gas is assumed here) and fuel (liquid assumed) flow rates. Similarly, the total mass flow rate is a summation of the oxidizer and fuel flow rates. The procedures for calculating these flow rates and their uncertainties are given in separate sections above. Here only the combined uncertainties for the mixture ratio and total mass flow are considered. (While the definitions given here presuppose that gaseous oxygen and a liquid hydrocarbon are being used, which is typical EC-1. However, the facility can also operate with gaseous hydrogen or hydrocarbons as fuels.)

MATHEMATICAL MODEL

The mixture ratio is defined as the ratio of oxidizer mass flow rate to fuel mass flow rate. The combined uncertainty is

$$u(MR) = MR\sqrt{\frac{u^2(\dot{m}_{ox})}{\dot{m}_{ox}^2} + \frac{u^2(\dot{m}_{fuel})}{\dot{m}_{fuel}^2}} \tag{25}$$

The combined uncertainty for the total mass flow rate is

$$u(\dot{m}_{total}) = \sqrt{u^2(\dot{m}_{ox}) + u^2(\dot{m}_{fuel})} \tag{26}$$

SOURCES OF UNCERTAINTY

The specific uncertainties are addressed in earlier sections and no additional complications arise when determining the mixture ratio or total mass flow rate. Again, the changes in values are largely a function of temperature. An increase in temperature increases the uncertainty in gas flow rate but decreases the uncertainty in liquid flow rate.

COMBINED UNCERTAINTY

Based on the numbers above and (25), the combined uncertainty in mixture ratio is between 15.9 and 0.76% dependant largely on the upstream gas temperature and the uncertainty of the thermocouple used to measure it. The main contributor to these uncertainties is the temperature, with uncertainty

Parameter	Source of Uncertainty	Uncertainty Value	Distribution of Uncertainty	Degrees of Freedom
Gas mass Flow Rate	Overall	9.77-0.56% Nanmac 15.9-1.88% Omega		
Liquid Mass Flow Rate	Overall	0.35-0.51%		
Mixture Ratio	Overall	9.78-0.76% Nanmac 15.9-1.95% Omega		
Total Mass Flow Rate	Overall	7.60-0.39% Nanmac 12.4-1.15% Omega		

Table 12. A breakdown of the mixture ratio and total mass flow uncertainty contributions. The gas flow rate uncertainty is given for a range of temperatures; the liquid mass flow rate is given for a single venturi with the range related to upstream pressure. Flow rates from 0.15-0.9 lb/s of gas and 0.10-0.35 lb/s liquid were considered with mixture ratios from 2.0 to 3.4. Trends are discussed in the combined uncertainty subsection.

decreasing as the propellant temperatures increases. At low temperatures the uncertainty in gas flow rate dominants the combined uncertainty; at 100°F the two flow rates contribute approximately equally.

For the total mass flow rate the overall uncertainty is between 12.4 and 0.39%. This uncertainty decreases with increasing temperature, but also has a sizeable increase as the mixture ratio increases., The gas flow rate always dominates the uncertainty, although at high temperatures and low mixture ratios it may be as low as 80% of the combined uncertainty.

BEST PRACTICES AND ADDITIONAL CONCERNS

The best practices listed for each of the mass flow rates apply. As there are no additional complications to determining this value, no additional discussion of best practices is needed.

AREA RATIO

BASIC PROCEDURE OVERVIEW

The area ratio is the ratio of combustion chamber area to the nozzle throat area. The nozzle throat area has been addressed above. The area ratio of the chamber is considered to be within the tolerances of the engineering drawing for the section. Note that prior to this analysis, the value used was the cross-sectional area of a square without rounded corners. This assumption results in 0.59 square inches of additional chamber area; in other terms, a 17% bias was introduced for the 2-inch section's area. Because the 1" sections are manufactured with a different technique, the rounding is the same as the tolerances, i.e. there is essentially no rounding, so the bias is substantially smaller in the 1" sections. Due to the ease of including the rounded corners in the area calculations, newer calculations make this correction.

MATHEMATICAL MODEL

The combined uncertainty in the area ratio is

$$u(AR) = AR\sqrt{\frac{u^2(A_c)}{A_c^2} + \frac{u^2(A_t)}{A_t^2}} \tag{27}$$

The area of the chamber is calculated as a square of width W minus the area left due to rounding the corners (W^2-$3\pi r^2$). The uncertainty in chamber area, then, is

$$u(A_c) = 2\sqrt{W^2u^2(W) + 9\pi^2r^2u^2(r)} \tag{28}$$

SOURCES OF UNCERTAINTY

The specific uncertainties in the throat area measurements are addressed in an above section. The uncertainty in the throat area and its components has been discussed above. Its combined uncertainty value is given in Table 12 for easy reference.

The in-house machine shop verifies the engine sections are within the tolerances prior to their use. However, during use some melting (especially of spool-section edges) and misalignment of the sections has been known to occur. These changes produce additional uncertainties beyond those captured by the tolerances. Unfortunately, no systematic measurements after testing have been conducted to date. For this current work, then, the uncertainty will be that introduced from the allowable tolerances on the engine sections. This uncertainty may be substantially smaller than the uncertainty actually encountered.

There are no additional complications or uncertainties in the area ratio beyond those captured in the individual area measurements.

Parameter	Source of Uncertainty	Uncertainty Value	Distribution of Uncertainty	Degrees of Freedom
Throat Area	Overall*	1.52-2.31 x 10^{-4} $inch^2$		
Chamber Width	Tolerance	0.004 inch		
Chamber Corner Radius	Tolerance	0.002 inch		
Chamber Area	Overall	0.01857 $inch^2$		
Area Ratio	Overall	0.1185-0.0564 (0.55%)		

Table 13. A breakdown of the area ratio uncertainty contributions. The results are for throat diameters from 0.45 to 0.65 inches and for the 2" chamber sections. Uncertainty for the chamber area of the 1 inch section is ~0.02 $inch^2$ based on tolerances which results in approximately 2.0% uncertainty for the area ratio.

COMBINED UNCERTAINTY

The combined uncertainty in area ratio is ~0.55%. With the current throat measurement techniques, the uncertainty in the throat area is the (much) smaller contributor to the combined uncertainty. The assumptions used to calculate the chamber area uncertainty likely underestimate this value, so the reported combined uncertainty is almost certainly too low.

BEST PRACTICES AND ADDITIONAL CONCERNS

Best practices for throat area determination are given above. Engine cross-sectional area can be improved by considering the true shape of the engine, not assuming it is square. Upon completion of a test series, the engine sections should be reassess to determine if their dimensions have changed. While this step is unlikely to do much to lower the uncertainty, it will provide a more believable value of that uncertainty. Also to be considered here is the fact that the engine cross-section likely does not stay constant throughout the test in this heat-sink hardware. However, it is unclear how to estimate deformations which might be occurring during the test.

STOICHIOMETRIC COEFFICIENTS

BASIC PROCEDURE OVERVIEW

The CEA code requires a chemical formula for the fuel [12]. Because EC-1 typically uses RP fuels (kerosene), an exact chemical formula is not available. Instead, the hydrogen and carbon weight percentages are measured, and these are used to determine the stoichiometric coefficients. These percentages are measured using the ASTM D5291 method B standard [27]. The machine used for the analysis is a Perkin Elmer EA2400 series II. The method that the machine uses is based on the Pregl-Demas method where fuels are combusted in pure oxygen and the resultant combustion gases are measured using gas chromatography.

MATHEMATICAL MODEL

The amount of carbon and hydrogen are both separately recorded as percentages of the initial weight of the sample. Given the specification for RP fuels, particularly RP-2 which is the standard fuel in EC-1, the weight of contaminants (i.e., species which are not carbon or hydrogen or contain other molecules in addition to carbon and hydrogen) are considered negligible. However, there may be some uncertainty associated with this assumption, so a value for the contaminants is included in the mathematical formulation.

There are several ways in which the chemical formula can be determined from reports of hydrogen and/or carbon percentages. Because the contaminants are assumed to be negligible, the

chemical formula could be related to the hydrogen (or carbon) percentage alone. As can be seen from the sources of uncertainty section below, the uncertainty in hydrogen percentage is lower, so if a single reported value is used, hydrogen is the best choice. The form of the assumed chemical formula also has flexibility. Some examples are C_xH_1, C_1H_x or C_xH_{2x+2} where *x* is a stoichiometric coefficient calculated from the measured percentage. A quick analysis indicates C_xH_1 is the best (lowest uncertainty) choice leading to an uncertainty in stoichiometric coefficient of

$$u(x) = x\sqrt{\frac{u^2(H\%)}{H\%^4(1-H\%)^2} + u^2(j) + \frac{u^2(MW_C)}{MW_C^2} + \frac{u^2(MW_H)}{MW_H^2}} \tag{29}$$

where $u^2(j)$ is the uncertainty associated with the contribution to total mass by the contaminants. The uncertainties in the molecular weight will be considered negligible (discussed in the enthalpy section), but are included in (29) for completeness.

Another way to determine the stoichiometric coefficients is from both the carbon and hydrogen percentages using a chemical formula C_xH_y. In this case, *x* and *y* are equal to the carbon and hydrogen percentages multiplied by the molecular weight of the other species. Or, *y* can again be set to one so that

$$x = \frac{MW_H C\%}{MW_C H\%} \tag{30}$$

(If *x* is set to unity instead of *y*, then *y* is the inverse of *x* given in (30).) In these formulations, where both carbon and hydrogen percentages are used, any contaminant percentage is already accounted for, so it does not need to be added to the uncertainty. If the value of *y* is set to 1, the uncertainty in *x* is

$$u(x) = x\sqrt{\frac{u^2(C\%)}{C\%^2} + \frac{u^2(H\%)}{H\%^2} + \frac{u^2(MW_C)}{MW_C^2} + \frac{u^2(MW_H)}{MW_H^2}} \tag{31}$$

Again, the molecular weights are included for completeness of formation—their contribution will be considered negligible. Note that the uncertainty for *y* if C_1H_y is used is similar to (31), but *y* is substituted for *x* in both sides of the equation.

Both equations (29) and (31) will be considered for determining the combined uncertainty. Also presented in Table 14 are the uncertainties considering both the C_1H_y or the C_xH_1 formulations. Both are considered because, as will be shown later, the enthalpy uncertainty depends on the stoichiometric coefficients, so minimizing the uncertainty in these coefficients may not minimize the uncertainty in enthalpy. If this contradiction occurs, the sensitivity analysis of the CEA code to the inputs must then be relied upon to determine which is more important—minimizing uncertainty in stoichiometric coefficients or minimizing uncertainty in enthalpy of formation.

SOURCES OF UNCERTAINTY

Per ASTM D5291 a total mass of 2 to 4 mg must be measured to +/-0.02 mg. Given the available balances and procedures at AFRL, this accuracy is achieved; the potential variability in total mass is considered as part of the repeatability and reproducibility given in the standard. These repeatability and reproducibility uncertainties of the process are listed in Table 14 below. ASTM reports user bias is not measurable and no bias was found between the four methods given in the standard. To achieve the accuracies noted in Table 14, the mass percentage of carbon must be between 75 and 87% and the mass percentage of hydrogen must be between 9 and 16%. The fuels used in EC-1 fall within this range, especially kerosene fuels such as RP-2 (typically given as around 85.5% carbon, 14.5% hydrogen).

The instrument used to measure the samples has a reported accuracy of <=0.3% and a reported precision of <=0.2%. These numbers are given by Perkin Elmer for “He carrier gas with certified standards”. Several other manufacturers report identical uncertainties in their instruments. Given the way in which the ASTM uncertainties are established [5] (i.e., through interlaboratory testing) it is assumed that these equipment uncertainties are considered within the cited reproducibility and repeatability numbers.

The amount of contaminants and the uncertainty they introduce is generally not known. The specifications for both RP-1 and RP-2 give boundaries on specific types of contaminants such as sulfur and particulates. However, in hydrogen and carbon percentage measurements contaminants encompass a broader range of substances—anything which does not break down into carbon and hydrogen. Experience at AFRL has shown that these other contaminants, such as molecules containing nitrogen and oxygen, are present in RP-2 at extremely low, often unmeasurable, levels. However, other fuels may have larger levels of contaminants. It is difficult to place a number on uncertainty associated with the assumption that no measurable level of contaminants exists. The percentage change in uncertainty of the stoichiometric coefficient produced from neglecting these components is less than the percentage (by weight) of the contaminant present for levels up to 2%. For example, if 2% of the total molecular weight (of a fuel which was nominally 14.5% H and 85.5% C) was due to contaminants, the uncertainty in stoichiometric coefficient would be off by 1.9%; if 0.5% of the molecular weight was contaminant then the uncertainty would change by 0.12% error would occur. Because the contaminant level is below measureable values, and its contribution to the uncertainty is similar to its value, the contribution to uncertainty will be neglected in the current analysis. With the assumptions that uncertainties in molecular weight and due to contamination are negligible, the uncertainty in stoichiometric coefficient when only considering H% reduces to

$$u(x) = \frac{xu(H\%)}{H\%^2(1-H\%)} \tag{32}$$

This reduction is nice because it applies to the case with C_1H_y as well by substituting *y* for *x* in the equation. With (32), it becomes clear that the uncertainty when calculating *x* is lower than the uncertainty if calculating *y* because the stoichiometric coefficient for the heavier, carbon, atom will always be smaller than that for the lighter, hydrogen, atom. Therefore, using the C_xH_1 formulation will minimize uncertainty in stoichiometric coefficient. As mentioned above, however, this selection will be revisited in the enthalpy section because the calculation of that value depends on the stoichiometric coefficients.

COMBINED UNCERTAINTY

The overall uncertainty in hydrogen percentage is $0.2589\sqrt{H\%}$ and in carbon percentage is 0.0194(C%+48.48). For the typical value of 14.5% hydrogen and 85.5% carbon, this works out to an uncertainty just under 1 percent of the 14.5% for the hydrogen and 2.6 percent of the 85.5 for carbon. The uncertainty in the stoichiometric coefficient x, again assuming 14.5% hydrogen, is 0.2714 if only H% is considered and 0.0369 if both H% and C% are considered. These values assume a formulation like C_xH_1. For the alternate formulation, C_1H_y, the uncertainties are 1.108 and 0.1505, again assuming 14.5%

Parameter	**Source of Uncertainty**	**Uncertainty Value**
Hydrogen %	Repeatability	$0.1162\sqrt{H\%}$
Hydrogen %	Reproducibility	$0.2314\sqrt{H\%}$
Hydrogen %	Total	$0.2589\sqrt{H\%}$
Carbon %	Repeatability	0.0072(C%+48.48)
Carbon %	Reproducibility	0.018(C%+48.48)
Carbon %	Total	0.0194(C%+48.48)
x (H% only)	Total	$0.02589x/\left[(1-H\%)H\%^{3/2}\right]$
x (H and C%)	Total	$x\sqrt{6.703\text{x}10^{-2}/H\% + 3.764\text{x}10^{-4}(1+48.48/C\%)}$
y (H% only)	Total	$0.02589y/\left[(1-H\%)H\%^{3/2}\right]$
y (H and C%)	Total	$y\sqrt{6.703\text{x}10^{-2}/H\% + 3.764\text{x}10^{-4}(1+48.48/C\%)}$

Table 14. The specific and combined uncertainties for the stoichiometric coefficients. The uncertainties are given for two different formulations, C_xH_1 and C_1H_y, and using either just the hydrogen percentage or both the hydrogen and carbon percentages. (Note that H and C% should be the values as percentages, so 14.5% hydrogen would be entered as 14.5 and not as 0.145. Similarly, results of the equations are percentages (they need not be multiplied by 100).)

hydrogen. The first value uses only H%; the second both H% and C%. So, if only the H% is used, the uncertainty in stoichiometric parameter at 14.5% hydrogen is 55%, but it is only 7.4% if both the hydrogen and carbon percentages are used. As implied by the finding that the equation for the uncertainties of *x* and *y* are essential identical, while the overall uncertainty in *y* is larger than *x* for the two formulations the uncertainty expressed as a percentage of the value is identical.

Despite being the smaller specific uncertainty, the uncertainty in hydrogen percentage is responsible for the majority (>80% for a typical range of compositions) of the combined uncertainty in stoichiometric coefficient if both species concentrations are considered. This dependence is due to the sensitivity coefficients and the fact that the hydrogen is the minor species by weight percentage. However, there were no techniques found to improve the uncertainty in hydrogen percentage. A major improvement in uncertainly can be made by using both the carbon and hydrogen percentage to calculate the stoichiometric coefficients, especially if the fuel has a large molecular weight contribution from contaminants. For fuels with minor contaminants, the resultant formulations will be identical regardless of whether both the hydrogen and carbon or just the carbon percentage is used, but this finding highlights the interesting nature of sensitivity coefficients and stresses the need to know the percentage of contaminants to develop an accurate formulation despite earlier findings that its contribution is small (i.e., it has a small effect on a large uncertainty which means while it may be neglected in the calculation of uncertainty, it is still important in the calculation of the stoichiometric parameter itself.)

BEST PRACTICES AND ADDITIONAL CONCERNS

Several instruments and processes were considered for determining the hydrogen and carbon percentages. A process superior to the one selected was not found. The instrumental uncertainty given here appears to be the industry standard. Selected instruments should have provisions which enable complete combustion (such as sample preheat) and good homogenization of product gases as these are the two largest contributors to uncertainty [27].

CEA has a default value for RP-1 [12]. These vary with different versions. In general, however, the defaults appear to have slightly lower hydrogen percentages (~14%) and larger enthalpy of combustion values (a few kJ/g larger) than those measured for the fuels in recent use in EC-1. Since, kerosene is a blended fuel and composition varies from batch to batch this variation is not surprising. It is good practice to evaluate samples and not rely on the default value.

With these considerations in mind the following steps are recommended

- Hydrogen and carbon percentages should be measured for each batch of fuel used.
  - They should be reported as individual percentages, as addressed here, not as a C-H ratio. This reporting scheme is not recommended in the ASTM standard and needlessly introduces extra complexity to the problem.
- The measuring process should be that described in ASTM D5291. Uncertainties are the same for any of the methods A, B, C and D given in the standard.
- Select an instrument which addresses the ability to enable complete combustion and, if method B or C is used, good homogenization of the combustion products
- The form of the equation should be C_xH_1 to minimize uncertainty in stoichiometric coefficient (percent uncertainty in parameter is the same regardless of formulation between C_xH_1 and C_1H_y). Note, however, that this does not necessarily minimize the uncertainty in theoretical c* due to the dependence of enthalpy on stoichiometric coefficients!
- Uncertainties can be lowered, by considering both the hydrogen and carbon percentages (in (30)) to calculate the stoichiometric coefficient. Given that the instrument and D5291 method already produce carbon percentage and the improvement in the event of contaminant species there is obvious no reason carbon percentage should not be measured.

ENTHALPY

BASIC PROCEDURE OVERVIEW

CEA requires the enthalpy (of formation) or internal energy of the reactants [12]. The enthalpy is used for EC-1 calculations. The heat of combustion is measured and used to determine the fuel's enthalpy of formation. The ASTM D4809 method is used to measure the heat of combustion [28]; this method is a bomb calorimeter technique designed for high precision measurements of the heat of combustion of fuels. All standards of the method are adhered to by the in-house analytical chemistry laboratory which performs the measurements. The enthalpy of formation is calculated from the heat of combustion using standard relations as detailed in the mathematical model section below.

MATHEMATICAL MODEL

From the basic definitions of heat (enthalpy) of combustion and formation and the generalized chemical formula of C_xH_y for a hydrocarbon fuel, the relation to get the enthalpy of formation of the fuel is

$$\Delta H_{f,fuel} = \Delta H_{comb}\left(MW_{fuel}\right) + x\Delta H_{f,CO2} + \frac{y}{2}\,\Delta H_{f,H2O} \tag{33}$$

Per the D4809 standard, the heat of combustion is reported as MJ/kg and must be multiplied by molecular weight to get the J/mol units needed for the CEA input. The net heat of combustion is typically reported, so the heat of formation for water in its gaseous form should be used in the above equation. (If the gross heat of combustion is used, then the heat of formation of the liquid state is the appropriate value.)

The combined uncertainty in enthalpy of formation of C_xH_y is

$$u\left(\Delta H_{f,fuel}\right) = \sqrt{\begin{array}{c} MW_{fuel}^2 u^2(\Delta H_{comb}) + x^2 u^2\left(\Delta H_{f,CO2}\right) + \frac{y^2}{4} u^2\left(\Delta H_{f,H2O}\right) \\ +(y\Delta H_{comb})^2 u^2(MW_H) + (x\Delta H_{comb})^2 u^2(MW_C) \\ +\left(MW_H^2 \Delta H_{comb}^2 + \frac{\Delta H_{f,H2O}^2}{4}\right) u^2(y) + \left(MW_C^2 \Delta H_{comb}^2 + \Delta H_{f,CO2}^2\right) u^2(x) \end{array}} \tag{34}$$

If a C_xH_1 formulation is used, y=1 and $u(y)$=0 in the above relation; if the C_1H_y formulation is used, x=1 and $u(x)$=0.

SOURCES OF UNCERTAINTY

The uncertainties cited in D4809 are for the entirety of the test method and typical equipment. The method deals with accuracies and procedures throughout the process. It is imperative that steps be taken to ensure complete combustion of the sample. The reader is referred to the standard for additional details [28]. Again, the net heat of combustion is reported and uncertainties related to this value are the ones cited in Table 15.

The uncertainties in stoichiometric coefficients are discussed above. The final combined uncertainties are reproduced in Table 15. As above, *y* will be set to unity and the uncertainty in *y* is zero for one set of calculations. The other formulation will also be considered with *x* set to one and the uncertainty in *x* set to zero.

Values and uncertainties in atomic weights of hydrogen and carbon and enthalpy of formation of carbon dioxide and (gaseous) oxygen are available from the literature. Generally, the uncertainties in these values are substantially lower than uncertainties in heat of combustion and stoichiometric coefficients, and the uncertainties in atomic weights and enthalpies of formation may be neglected. From NIST webbook [21] the heats of formation are -241.826 +/- 0.040 kJ/mol for water and -393.51 +/- 0.13 kJ/mol for carbon dioxide. A recent paper reports the atomic weights of hydrogen and carbon as 1.00794 +/- 0.00007 g/mol and 12.0096 +/- 0.0008 g/mol respectively [29]. Comparing these values to those related to the heat of combustion and stoichiometric coefficients, their contributions to the combined

uncertainty indicate that they are negligible. Neglecting these values and simplifying the combined uncertainty gives

$$u(\Delta H_{f,fuel}) = \sqrt{MW_{fuel}^2 u^2(\Delta H_{comb}) + \left(MW_H^2 \Delta H_{comb}^2 + \frac{\Delta H_{f,H2O}^2}{4}\right) u^2(y) + \left(MW_C^2 \Delta H_{comb}^2 + \Delta H_{f,CO2}^2\right) u^2(x)} \quad (35)$$

(35) helps to showcase an interesting difficulty. Either the uncertainty in *y* is zero or the uncertainty in *x* is zero, depending on how the chemical formulation is calculated. The combined uncertainty in *x* is always smaller than the combined uncertainty in *y*, as shown in the previous section. However, when calculating the enthalpy the sensitivity coefficient for *x* is a combination of the heat of formation of carbon dioxide and the atomic weight of carbon while the sensitivity coefficient for *y* is composed of the smaller heat of formation of water and atomic weight of hydrogen. The comparison of values is partially offset by the molecular weight of the fuel being lower for C_xH_1 than for C_1H_y. However, as shown in Table 15, the sensitivity factors are sufficient to produce a larger uncertainty when C_xH_1 is used, despite the uncertainty in stoichiometric coefficient being smaller with this formulation. Final assessment on the preferred formulation will need to consider the sensitivity coefficients of the CEA code, discussed in a later section.

Parameter	**Source of Uncertainty**	**Uncertainty Value**
Heat of Combustion	Repeatability	0.099 kJ/g
Heat of Combustion	Reproducibility	0.234 kJ/g
Heat of Combustion	Bias	0.089 kJ/g
Heat of Combustion	Total	0.269 kJ/g
x (H% only)	Total	0.2714
x (H and C%)	Total	0.0369
y (H% only)	Total	1.1083
y (H and C%)	Total	0.1505
Enthalpy of Formation (x) (H% only)	Total*	177.8 kJ/mol (1422%)
Enthalpy of Formation (x) (H and C%)	Total*	24.22 kJ/mol (194%)
Enthalpy of Formation (y) (H% only)	Total*	142.6 kJ/mol (564%)
Enthalpy of Formation (y) (H and C%)	Total*	19.73 kJ/mol (78.1%)

Table 15. The specific and combined uncertainties for the enthalpy of formation. The uncertainties are given for two different formulations, C_xH_1 and C_1H_y, and using either just the hydrogen percentage or both the hydrogen and carbon percentages. These values use the heat of combustion and composition reported for Sample ID: RP2 20081229—43.61 MJ/kg, 14.5% H and 85.5% C.

COMBINED UNCERTAINTY

The combined uncertainty for the enthalpy of formation of C_xH_1 is 177.8 kJ/mol using only H% or 24.22 kJ/mol using both H and C% for calculating the stoichiometric coefficients. These values are 1422 and 171% of the calculated enthalpy, respectively. For C_1H_y the values are moderately better, 142.6 kJ/mol and 19.73 kJ/mol; the percentage uncertainty is substantially improved, however, to 564% and 78.1%. Clearly, then using the C_1H_y formulation produces the lowest uncertainty in enthalpy. Again, this finding is opposite that for the values of the uncertainties in stoichiometric coefficients where a C_xH_1 formulation is recommended (percentage uncertainties are identical). These values are given for a specific fuel with a measured heat of combustion of 43.61 MJ/kg and 14.5% hydrogen, 85.5% carbon. A lower H% or a larger heat of combustion produces a greater uncertainty (and percentage uncertainty).

The uncertainty in the stoichiometric coefficients dominates the combined uncertainty; this is due to their large sensitivity coefficients. As stated in the section on stoichiometric coefficients, there are few ways to further reduce this uncertainty beyond considering both the hydrogen and carbon percentages (again recommended here).

BEST PRACTICES AND ADDITIONAL CONCERNS

The ASTM standard (D4809) outlines best practices for conducting the heat of combustion measurements. Using a C_1H_y formulation minimizes the uncertainty in enthalpy of formation. This is the opposite of the findings for stoichiometric coefficient. Still, both the hydrogen and carbon percentage should still be used in determining the stoichiometric coefficients regardless of the formulation used. A look at sensitivity coefficients in CEA, following, is needed to determine which formulation to use.

SENSITIVITIES OF CEA TO INPUTS

As indicated above, the inputs to CEA are the area ratio (chamber to nozzle), the mixture ratio, the stoichiometric coefficients, the enthalpy of formation of the fuel, the chamber pressure and the temperature of the reactants [12]. The uncertainties of each of these parameters are addressed above. Under typical operation in EC-1, a test is performed and the measured mixture ratio, chamber pressure and temperature of the reactants are entered into a CEA routine which already contains the other parameters—these other parameters are invariant unless the hardware or fuel is changed.

The current approach to the determination of the sensitivity parameters is still in progress, so a simple process for a single set of “representative” values is all that is considered. More robust analysis will be carried out in the future.

To determine the sensitivities, a typical set of values is chosen for all the inputs. A range is then determined from the uncertainty analysis. The values and ranges are listed in Table 16. CEA calculations were performed holding all but one parameter at its nominal value. The variable parameter was divided into 6 to 12 points covering the range (plus and minus the single-sided range). Once the c*-efficiency has been calculated from CEA for the full range of one parameter, a line is fit through the results (c* versus varying parameter). The slope of the resulting line is the sensitivity coefficient. In the case of temperature, the results were not linear over the range, so the range was increased and two equal-length lines were fit to the step-wise linear results. Both slopes were very similar; the maximum is used here. It is assumed in this process that all inputs and uncertainties are independent. The analysis of the enthalpy, for example, shows that this assumption is incorrect as does the analysis of mixture ratio with regards to temperature. So this simple analysis neglects covariances and other complexities. Future analysis will consider the relation between inputs [30]. The current analysis gives basic insight into the relative contribution of each parameter in a simple, straightforward way.

Parameter	Uncertainty Range	Varies with	Range
Pressure	0.0919 to 0.0181%	Increases with P	300-2000 psi
Throat Area	0.0958 to 0.0696%	Increases with Dt	0.45 to 0.65 inch
Mass (Nanmac)	5.864 to 7.647%	Increases with mass	0.25-1.15 lb/s @ 40°F
Mass (Nanmac)	0.3943 to 0.4524%	Increases with mass	0.25-1.15 lb/s @ 100°F
Mass (Omega)	9.541 to 12.44%	Increases with mass	0.25-1.15 lb/s @ 40°F
Mass (Omega)	1.147 to 1.476%	Increases with mass	0.25-1.15 lb/s @ 100°F
Characteristic Velocity	5.864 to 7.648% 0.4161 to 0.4715%		Nanmac @ 40°F Nanmac @ 100°F
Characteristic Velocity	9.542 to 12.44% 1.154 to 1.482%		Omega @ 40°F Omega @ 100°F

Table 17. The uncertainties and ranges considered for the measured characteristic velocity.

Parameter	Nominal Value	Single-Sided Range	# Points	Sensitivity	Uncertainty
Mixture Ratio	2.4	0.25	10	185.6	0.0375 Nanmac 0.0812 Omega
Area Ratio	21.4	0.12	6	At the limit of resolution, 0.4 maximum	0.1185 inch
Stoichiometric Coefficient (x)	0.49	0.04	8	290.62	0.036858 (C & H%)
Stoichiometric Coefficient (y)	2.04	0.15	6	0 within resolution	0.1505 (C & H%)
Enthalpy of Formation (x)	-12.5 kJ/mol	12 kJ/mol	12	0.0114	24.2 kJ/mol
Enthalpy of Formation (y)	-25.3 kJ/mol	20 kJ/mol	10	0.0056	19.7 kJ/mol
Chamber Pressure	700 psi	0.3 psi	12	0.2058	0.28629 psi
Reactant Temperature	77°F	2.25°F	9	0.1814 (all from gas)	0.4491°C Nanmac 1.0021°C Omega

Table 16. The values, range, number of points and sensitivity for a single, hypothetical experiment in EC-1.

C*-EFFICIENCY

COMBINED UNCERTAINTY

The combined uncertainty in the measured characteristic velocity is outlined in Table 17. The main contributor is the uncertainty in temperature which propagates through to the characteristic velocity through the gas mass flow rate to the total mass flow rate. Operating at elevated temperatures with the thermocouple uncertainty given by Nanmac produces a situation where the throat area and pressure may contribute up to 5% each to the total uncertainty percentage. It should be noted that typically EC-1 uses Nanmac thermocouples to measure the gas and liquid inlet velocity and, while the temperature can be as low as 40°F, the temperature is typically a more moderate 70°F or above. This smaller temperature range and lower thermocouple uncertainty result in combined characteristic velocity uncertainty under 2% over the range of pressures and throat areas.

The contributions to the uncertainty in theoretical characteristic velocity are given in Table 16 for a specific “nominal” case. The flow rates for this care are set to near median values of those considered in this preliminary analysis—0.5 lb/s of gas and 0.2083 lb/s of liquid. The combined uncertainty is 4.26 ft/s for the Nanmac thermocouples using a C_xH_1 formulation and 2.71 ft/s using a C_1H_y formulation. Clearly, then, gains can be made by choosing the C_1H_y formulation even though this increases the

uncertainty in stoichiometric coefficients. This result is actually not due to the lower uncertainty in enthalpy since the sensitivities vary between the formulations creating a similar contribution by enthalpy regardless of formulation. The main reason is that CEA shows much less sensitivity to changes in the number of hydrogen atoms as opposed to carbon atoms in a hydrocarbon. The main contributor to the uncertainty in theoretical c* is the mixture ratio. The uncertainty in mixture ratio is again dominated by the uncertainty in gas flow rate and, through it, temperature. (Combined uncertainties for the Omega thermocouples are 5.13 and 3.95 ft/s depending on formulation.) For reference, the theoretical characteristic velocity at the nominal conditions given in Table 16 is 5064.7 ft/s for a C_xH_1 and 5066.0 ft/s for the other formulation. Considering the four permutations here, the uncertainty is always under 0.1%

Combining these uncertainties in each characteristic exhaust velocity along with (3) results in an overall, combined uncertainty of 1.21% of the c*-efficiency using the Nanmac thermocouples and 2.44% using the Omega thermocouples. This value is for a specific set of conditions listed in Table 17; when measurements are made at lower temperatures, this uncertainty will increase dramatically. In general, the combined uncertainty in efficiency is dominated at this condition by the measured c*. Although the current sensitivity analysis for calculating the uncertainty in theoretical c* is still rough, the calculations indicate that it is substantially smaller than its measured counterpart. At present, the uncertainty in the measured characteristic value gives a reasonable estimate of the combined uncertainty in efficiency. Therefore, a range from nearly 8% to under 1% based on propellant temperature could be reasonable expected.

CONCLUSIONS

BEST PRACTICES AND ADDITIONAL CONCERNS FOR OVERALL C-EFFICIENCY*

Examination of Figs. 26 and 27 indicates that <a and b> are the largest contributors to the uncertainty in each *c** measurement. Best practices for individual measurements contributing to the c*-efficiency are given in individual sections above. However, a few findings are applicable to multiple measurements or in general

- The temperature and pressure are important in many measurements as well as on their own. Every effort should be taken to minimize their uncertainties.
- Frequent and careful calibrations are of utmost importance to maintain low uncertainty.
  - The calibration results should be checked with the expected uncertainties. If values fall outside of uncertainty bands (with some confidence interval), the uncertainty in previous measurements must be increased, reasons for the discrepancy should be investigated and, likely, a more-frequent calibration schedule should be used
- Use ASTM, ISO, etc. standards for measurement techniques when available. These tend to have the lowest repeatability and overall uncertainty reasonably achievable and produce easily traceable uncertainty results.

The development of this document has helped to guide and improve the practices and equipment in the EC-1 facility. This in-depth analysis has also illustrated that uncertainty determination for small-scale engines is quite complex. Given the great lengths taken to minimize uncertainties here and the results as compared with results presented in the industry literature, it seems probable that uncertainties in the literature are often underestimated likely due to simplifying the analyses

FUTURE WORK

While this paper attempts a complete, in-depth analysis of the uncertainty in a small-scale engine, it is not yet complete. For several measurands only a single, randomly chosen device was analyzed here. Information on uncertainty distributions and degrees of freedom remain to be determined for many of the uncertainties. Without these, no confidence intervals can be calculated. The heat transfer corrections for the efficiency also need to be considered along with their uncertainty propagation to the overall c*-efficiency. The vapor pressure uncertainties and effect of neglecting pressure when calculating

the fuel density also need to be examined in additional detail. Finally, the sensitivity coefficient determination for the theoretical c^* inputs will be expanded to a more robust and complete formulation.

Several corrective and improved practices also remain to be implemented into the EC-1 procedures. These include such things as analysis and correction of the temperature dependence of the pressure transducers and manometer and correction of the chamber pressure for losses along the engine length and from static to stagnation. Additional, better on-going monitoring of the cross-sectional area of the engine sections will be added to the current operational procedures. Of utmost importance, however, will be a further investigation of thermocouple uncertainty and the possibility of using different measuring devices to improve the uncertainty in temperature. This uncertainty is by far the largest remaining uncertainty.

Despite this large list of future work, a major part of the work and analysis has already been completed. Future work will serve to clarify and improve the uncertainty in the EC-1 facility.

REFERENCES

1. Cohn, R.K., S.A. Danczyk, and R.W. Bates, *A Comparison of the Performance of Hydrocarbon Fuels in a Uni-element Combustor*, AIAA 2003-4752, in *39th AIAA/ASME/SAE/ASEE Joint Propulsion Conference and Exhibit*. 2003: Huntsville, AL.
2. *Measurement Uncertainty Analysis Principles and Methods*, NASA HDBK-8739.19-3, 2010.
3. ISO, *Evaluation of Measurement Data -- Guide to the Expression of Uncertainty in Measurement*, JCGM, 100:2008, 2008.
4. Taylor, B.N. and C.E. Kuyatt, *Guidelines for Evaluating and Expressing the Uncertainty of NIST Measurement Results*, NIST 1297, 1994.
5. ASTM International, *Standard Guide for Statistical Procedures to Use in Developing and Applying Test Methods*, ASTM E1488, 2009.
6. American Institute of Aeronautics and Astronautics, *Assessing Experimental Uncertainty-Supplement to AIAA S-071A-1999*, AIAA-G-048-2003, 2003.
7. *JANNAF Rocket Engine Performance Test Data Acquisition and Interpretation Manual,* CPIA 245, 1975.
8. Miller, K., et al., *Experimental Study of Combustion Instabilities in a Single-Element Coaxial Swirl Injector*, AIAA 2005-4298, in *41st AIAA/ASME/SAE/ASEE Joint Propulsion Conference and Exhibit*. 2005: Tucson, AZ.
9. Mulkey, H.W., M.D. Moser, and M.A. Hitt, *GOX/Methane Combustion Efficiency of a Swirl Coaxial Injector*, AIAA-2009-5141, in *45th AIAA/ASME/SAE/ASEE Joint Propulsion Conference*. 2009: Denver, CO.
10. Santoro, R.J., et al., *Rocket Testing at University Facilities*, AIAA 2001-0748, in *39th AIAA Aerospace Sciences Meeting and Exhibit*. 2001: Reno, NV.
11. Vaidyanathan, A., J. Gustavsson, and C. Segal, *Oxygen/Hydrogen-Planar-Laser-Induced Fluorescence Measurements and Accuracy Investigation in High-Pressure Combustion.* Journal of Propulsion and Power, 2009. **25**(4): p. 864-874.
12. McBride, B.J. and S. Gordon, *Computer Program for Calculation of Complex Chemical Equilibrium Compositions and Applications, II. Users manual and Program Description*, NASA-RP 1311, 1996.
13. Mathioulakis, E. and V. Belessiotis, *Uncertainty and traceability in calibration by comparison.* Measurement Science and Technology, 2000. **11**: p. 771-775.
14. Bjorklund, R.A., R.S. Rogero, and R.K. Baerwald, *Handbook of Recommended Practices for the Determination of Liquid Monopropellant Rocket Engine Performance*, Jet Propulsion Laboratory Publication 79-32, 1979.
15. Omega. *Thermocouple Wire and Thermocouple Cable*. [Available from: http://www.omega.com/prodinfo/thermocouplewire.html].

16. Coy, E.B., *Measurement of Transient Heat Flux and Surface Temperature Using Embedded Temperature Sensors.* Journal of Thermophysics and Heat Transfer. **24**(1): p. 77-84.
17. *Measurement of Plain External Diameters for use as Master discs or Cylindrical Plug Gages*, ASME B89.1.5, 1998.
18. Kipp, D.O., *Metal Material Data Sheets*. 2010, MatWeb - Division of Automation Creation, Inc.
19. ASTM International, *Standard Test Method for Density, Relative Density, and API Gravity of Liquids by Digital Density Meter*, ASTM D4052, 2009.
20. ASTM International, *Standard Test Method for Determination of Vapor Pressure of Crude Oil: VPCRx (Expansion Method)*, ASTM D3677, 2010.
21. Lemmon, E.W., M.O. McLinden, and D.G. Friend, *NIST Chemistry WebBook*, in *NIST Standard Reference Database Number 69*, P.J. Linstrom and W.G. Mallard, Editors. 2011, National Institute of Standards and Technology: Gaithersburg, MD.
22. *Integrated Pressure Systems*, Air Force T.O. 00-25-223, 2006.
23. ISO, *Measurement of fluid flow by means of pressure differential devices inserted in circular cross-section conduits running full* , ISO 5167, 2003.
24. Stewart, D.G., J.T.R. Watson, and A.M. Vaidya, *Improved critical flow factors and representative equations for four calibration gases.* Flow Measurement and Instrumentation, 1999. **10**: p. 27-34.
25. *CODATA Value: molar gas contant*. 2010 [Available from: http://physics.nist.gov/cgi-bin/cuu/Value?r|search_for=gas+contant].
26. Stewart, D.G., J.T.R. Watson, and A.M. Vaidya, *Effect of high beta values on mass flow through critical flow nozzles.* Flow Measurement and Instrumentation, 2000. **11**: p. 351-356.
27. ASTM International, *Standard Test Methods for Instrumental Determination of Carbon, Hydrogen, and Nitrogen in Petroleum Produces and Lubricants*, ASTM D5291, 2010.
28. ASTM International, *Standard Test Method for Heat of Combustion of Liquid Hydrocarbon Fuels by Bomb Calorimeter (Precision Method)*, ASTM D4809, 2009.
29. Pure Applied Chemistry, 2011. **83**: p. 359-396.
30. Oakley, J.E. and A. O'Hagan, *Probabilistic sensitivity analysis of complex models: a Bayesian approach* Journal of the Royal Statistical Society B, 2004. **66**(4): p. 751.